Zoe Bernasconi
MPMI

Mutagenesis of wheat powdery mildew reveals a single gene controlling both NLR and tandem kinase-mediated immunity

Zoe Bernasconi[1], Ursin Stirnemann[1], Matthias Heuberger[1], Alexandros G. Sotiropoulos[1,2], Johannes Graf[1], Thomas Wicker[1], Beat Keller[1*], Javier Sánchez-Martín[1,3*]

[1] Department of Plant and Microbial Biology, University of Zurich, Zurich, Switzerland

[2] Centre for Crop Health, University of Southern Queensland, Darling Heights, Queensland, Australia

[3] Department of Microbiology and Genetics, Spanish-Portuguese Agricultural Research Centre (CIALE), University of Salamanca, Salamanca, Spain

* Corresponding authors: Beat Keller; E-mail: bkeller@botinst.uzh.ch; Javier Sánchez-Martín; E-mail: j.sanchezmartin@usal.es

16 **Abstract**

17 *Blumeria graminis* f. sp. *tritici* (*Bgt*) is a globally important fungal wheat pathogen. Some
18 wheat genotypes contain powdery mildew resistance (*Pm*) genes, encoding immune
19 receptors that recognize specific fungal-secreted effectors proteins, then defined as
20 avirulence (Avr) factors. Identifying Avr factors is vital for understanding the mechanisms,
21 function, and durability of wheat resistance. Here, we present AvrXpose, an approach to
22 identify *Avr* genes in *Bgt* by generating gain-of-virulence mutants on *Pm* genes. We first
23 identified six *Bgt* mutants with gain of virulence on *Pm3b* and *Pm3c*. They all had point
24 mutations, deletions or insertions of transposable elements within the corresponding
25 *AvrPm3*$^{b2/c2}$ gene or its promoter region. We further selected six mutants on *Pm3a*, aiming
26 to identify the yet unknown AvrPm3^{a3} recognized by Pm3a, in addition to the previously
27 described AvrPm3$^{a2/f2}$. Surprisingly, *Pm3a* virulence in the obtained mutants was always
28 accompanied by an additional gain of virulence on the unrelated tandem kinase resistance
29 gene *WTK4*. No virulence towards 11 additional *R* genes tested was observed, indicating
30 that the gain of virulence was specific for *Pm3a* and *WTK4*. Several independently
31 obtained *Pm3a-WTK4* mutants have mutations in *Bgt-646*, a gene encoding a putative,
32 non-secreted ankyrin repeat-containing protein. Gene expression analysis suggests that
33 *Bgt-646* regulates a subset of effector genes. We conclude that *Bgt-646* is a common
34 factor required for avirulence on both a specific NLR and a WTK immune receptor. Our

35 findings suggest that, beyond effectors, another type of pathogen protein can control the

36 race-specific interaction between powdery mildew and wheat.

37 **Keywords**: AvrXpose, mutagenesis, effectors, avirulence factors, transposable elements,

38 *Blumeria graminis*, wheat, race-specific resistance, NLR, tandem kinase proteins

39 **Introduction**

40 Plant pathogens secrete effector proteins that interfere with host metabolism and
41 suppress its immune response (Dodds and Rathjen 2010; Lo Presti et al. 2015). Host
42 resistance (*R*) genes encode intracellular receptors that directly or indirectly recognize
43 pathogen effectors. This recognition results in effector-triggered immunity (ETI; Jones and
44 Dangl, 2006), and frequently culminates in a hypersensitive response (HR) and cell death.
45 Recognized effectors are also called avirulence (Avr) effectors and are considered
46 disadvantageous for the pathogen. Consequently, strong host resistance results in an
47 efficient selection for mutated (or deleted) effectors, or reduced effector expression to
48 avoid recognition (Lo Presti et al. 2015; Sánchez-Vallet et al. 2018). Thus, there is a trade-
49 off between avoidance of recognition and the loss of effector gene function, which could
50 result in a fitness cost (Sánchez-Vallet et al. 2018).

51 Powdery mildews form one of the most widespread group of plant pathogens, infecting
52 an estimated 10,000 plant species (Takamatsu 2004). Among them are crop plants,
53 including bread wheat, infected by wheat powdery mildew (*Blumeria graminis* f. sp. *tritici,*
54 *Bgt*) (Sánchez-Martín, Bourras, and Keller 2018). Powdery mildews are obligate biotrophic,
55 highly specialized pathogens that need living host tissue to proliferate. Previous work on
56 the wheat-*Bgt* pathosystem mostly focused on *R* genes encoding nucleotide-binding
57 leucine-rich repeat (NLR) immune receptors. One of the most studied NLR-encoding *R*
58 genes conferring resistance to *Bgt* is the allelic series *Pm3* (Yahiaoui, Brunner, and Keller

59 2006). It has been shown that different Pm3 allelic variants recognize sequence-unrelated
60 effectors of *Bgt*. Pm3a and Pm3f recognize the same Avr, AvrPm3$^{a2/f2}$ (Bourras et al. 2015),
61 while Pm3b and Pm3c recognize AvrPm3$^{b2/c2}$ (Bourras et al. 2019). *Pm3a* and *Pm3b* have
62 an extended resistance spectrum compared to their companion alleles, *Pm3f* and *Pm3c*,
63 respectively (Stirnweis et al. 2014). Brunner et al. (2010) tested a large set of *Bgt* isolates
64 and found that *Pm3a*-mediated resistance against 454 isolates, including all 173 isolates
65 avirulent on *Pm3f*, thus exhibiting an extended resistance spectrum compared to *Pm3f*.
66 Similarly, the *Pm3b* allele showed broader resistance than the narrow-spectrum *Pm3c*
67 allele. Genetic analysis in mapping populations suggested the existence of additional
68 pathogen components involved in different Pm3-AvrPm3 interactions, which may explain
69 the differences in the resistance spectra of the *Pm3* alleles (Bourras et al. 2015, 2016). The
70 *Pm3-AvrPm3* interaction is further complicated by the presence of a suppressor gene of
71 avirulence in some mildew isolates (*SvrPm3*; Bourras et al. 2015; Parlange et al. 2015),
72 which was proposed to encode a general factor involved in all AvrPm3-Pm3 interactions
73 by masking the presence of AvrPm3 effectors, thus blocking a resistance response. In
74 addition, *AvrPm3$^{a2/f2}$* is present in multiple copies in different *Bgt* isolates (Müller et al.
75 2019). *Pm3-AvrPm3* is not a unique case of a non-canonical gene-for-gene interaction: it
76 has been reported for other *R* genes, such as *Pm1a* (Hewitt et al. 2021; Kloppe et al. 2023),
77 that multiple pathogen components determine the interaction with the host.
78 In recent years, novel types of immune receptors have been described to confer race-
79 specific resistance in wheat (Sánchez-Martín and Keller 2021). These include, in the case

80 of wheat powdery mildew, tandem kinase proteins such as *Pm24* (Lu et al. 2020) and *WTK4*
81 (Gaurav et al. 2022), and other kinase-fusion proteins, such as *Pm4* (Sánchez-Martín et al.
82 2021). However, little is known about how these novel proteins function at the molecular
83 level. Rpg1, identified by Brueggeman et al. (2002), is the most studied tandem kinase
84 protein. It confers race-specific resistance to stem rust in barley and was observed to be
85 phosphorylated and degraded upon infection with avirulent rust spores. Two rust proteins,
86 a fibronectin type III and breast cancer type 1 susceptibility protein and a vacuolar protein,
87 were described as determinants of Rpg1 phosphorylation and hypersensitive response in
88 resistant cultivars (Nirmala et al. 2011). However, there is limited knowledge about the
89 recognition mechanisms of other tandem kinase or kinase-fusion proteins and the specific
90 pathogen components with which they interact (Klymiuk et al. 2021). The identification of
91 the Avr components recognized by unconventional R proteins is essential for
92 understanding the activation of the plant immune system by these novel immune
93 receptors.
94 All *Bgt* Avr effectors identified to date are small (less than 159 amino acids), have a signal
95 peptide, conserved cysteine residues at defined positions, and all share a predicted or
96 confirmed RNAse-like 3D structure (McNally et al. 2018; Bourras et al. 2016, 2019; Praz et
97 al. 2017; Cao et al. 2023). Genomic and transcriptomic GWAS, QTL mapping and effector
98 benchmarking have been used to identify *Avr* genes in cereal powdery mildews. However,
99 these methods have some limitations, such as the need to maintain and sequence large
100 populations, the bias given by the reference genome(s), and the requirement for genetic

101 variability and recombination at the *Avr* loci. The lack of stable transformation protocols
102 for *Bgt* further hampers *Avr* identification and characterization. In other classes of obligate
103 fungal pathogens, some attempts have been made to obtain mutants with gain of
104 virulence: for example, by ethyl-methane sulfonate (EMS) treatment in wheat rusts and
105 barley powdery mildew (Sherwood, Slutsky, and Somerville 1991). EMS mutagenesis
106 allowed the identification of *AvrSr35* in stem rust (Salcedo et al. 2017) while spontaneous
107 mutants contributed to the identification of *AvrSr50* (Chen et al. 2017) and *AvrSr27*
108 (Upadhyaya et al. 2021). Recently, ultraviolet light (UV) mutagenesis has been used in
109 quasi-evolutionary experiments to study induced mutations involved in fungal viability
110 and pathogenesis in barley powdery mildew (Barsoum et al. 2020), but mutagenesis has
111 not been used to identify *Avr* factors in cereal powdery mildews.
112 In this work, we aimed to establish a methodology to identify *Avr* factors using UV
113 mutagenesis to circumvent some limitations of the other *Avr* identification approaches. As
114 a proof of concept, we first demonstrate the efficiency of our approach by identifying six
115 and two mutants of the $AvrPm3^{b2/c2}$ and $AvrPm3^{a2/f2}$ avirulence genes, respectively,
116 revealing different molecular mechanisms of escape from recognition. Further, since
117 mutants virulent on *Pm3f* did not gain virulence on *Pm3a*, we used a *Pm3f*-virulent mutant
118 as a background to apply AvrXpose to the case of *Pm3a*, identifying six *Pm3a* virulent
119 mutants. Finally, we show that our approach can identify a pathogen factor controlling
120 avirulence on two different types of *R* genes, an *NLR* and a *WTK*. We conclude that classical

121 *Avr* effectors are only one type of pathogen factors contributing to the specificity of R-Avr

122 interactions.

123 **Results**

124 Gain-of-virulence *Bgt* mutants on *Pm3b* and *Pm3c* generated by ultraviolet mutagenesis
125 reveal different mechanisms of escape from recognition

126 We wanted to establish a pipeline based on UV irradiation to induce mutations in genes
127 controlling avirulence on different alleles of the *Pm3* gene. We developed an approach
128 which we named "AvrXpose". In three rounds, we mutagenized and propagated the *Bgt*
129 isolate CHE_96224, avirulent on all tested *Pm3* alleles, on the powdery mildew susceptible
130 line Kanzler. Mutagenized spore mixtures were then used to infect near-isogenic lines
131 (NILs) containing one of the *R* genes *Pm3a*, *Pm3b*, *Pm3c*, *Pm3d*, *Pm3f* or a transgenic line
132 containing *Pm3e* (E#2) to select *Pm3* allele gain-of-virulence mutants (**Figure 1**).

133 Since virulence to *Pm3c* was suggested to be determined by only one avirulence
134 component (*AvrPm3*$^{b2/c2}$; Bourras et al. 2015, 2019), we assumed that a gain of virulence
135 on *Pm3c* would result from a single mutation in the known *Avr*. Hence, we first tested the
136 feasibility of our method by identifying *AvrPm3*$^{b2/c2}$ mutants. In addition, we also wanted
137 to determine if it was feasible to obtain mutants virulent on *Pm3b*, since it shows broader
138 resistance than *Pm3c* (Stirnweis et al. 2014; Brunner et al. 2010). We obtained six
139 independent *Bgt* mutants with simultaneous gain of virulence on both *Pm3b* and *Pm3c*
140 (hereafter, 3BC mutants) by selecting them on wheat lines containing either *Pm3b* or *Pm3c*
141 (**Figure 2A**). Notably, the 3BC mutants remained avirulent on the other *Pm3* alleles tested
142 (*Pm3a*, *Pm3d*, *Pm3e* and *Pm3f*; **Supplementary Figure S1**). To further investigate the

143 specificity of the gain of virulence on other *Pm* resistance genes, we also infected NILs
144 containing *Pm1a*, *Pm2*, *Pm4a*, *Pm4b*, *Pm8, Pm24* and three *Aegilops tauschii* lines
145 containing *WTK4* with the mutants. We confirmed that the 3BC mutants were still avirulent
146 on them as well, with the exception of *Pm1a* and *Pm8*, for which the parental isolate
147 CHE_96224 is virulent (**Supplementary Figure S1**). This demonstrates that the mutants
148 are affected specifically in avirulence to *Pm3b* and *Pm3c*.
149 Next, we wanted to determine the genetic cause of the gain of virulence. Illumina whole-
150 genome sequencing followed by single nucleotide polymorphism (SNP) calling to the
151 wild-type, non-mutated *Bgt* isolate CHE_96224, revealed between 253 and 975 SNPs and
152 small (<7 bp) InDels per *Bgt* isolate (**Table 1**). Among these SNPs, 41 to 503 were unique
153 mutations, i.e., present only in one mutant of the same mutant group (**Table 1**,
154 **Supplementary Tables S1**, **S2**, **S3**). We observed that the discrepancy between total and
155 unique SNPs was mostly due to SNP calling artefacts. In transposable element (TE)-rich,
156 repetitive, or low sequencing depth regions, there was a certain level of heterozygosity
157 and ambiguous mapping in the reads of all *Bgt* mutants, which led to some wrong SNP
158 calling. Nonetheless, we eliminated most of these cases by filtering for unique mutations.
159 This issue was previously encountered by Barsoum et al. (2020), who also filtered
160 mutations by uniqueness and visually inspected all variants individually to exclude false
161 positives.
162 Additionally, we searched for gene deletions by examining the average depth of
163 sequencing coverage as well as TE insertions using the TE detection software *detettore*

164 (Stritt and Roulin 2021). We then compared all the variants from the six mutants with each
165 other and examined the mutation overlap.
166 All 3BC mutants had a mutant variant in (or near) the known *AvrPm3*$^{b2/c2}$ gene (**Figure 2A**,
167 **Supplementary Table S4**). Mutant 3BC_1 had a 1 base pair (bp) deletion in the gene's
168 coding sequence, causing a frameshift and a premature STOP codon at amino acid
169 position 67. Sequence coverage analysis showed that mutant 3BC_2 had a 9.5 kb
170 chromosomal deletion where the *AvrPm3*$^{b2/c2}$ gene is embedded (**Supplementary Table**
171 **S4**). *Detettore* revealed that mutants 3BC_3 and 3BC_4 both had insertions of *RII_Itera*
172 family non-LTR retrotransposons between 467 and 470 bp upstream of the ATG start
173 codon of *AvrPm3*$^{b2/c2}$ (**Figure 2A, Table 2**). By *de-novo* assembling the *AvrPm3*$^{b2/c2}$ locus
174 in both mutants, we confirmed that they had independent TE insertions, because mutant
175 3BC_4 had an 80 bp DNA fragment from chromosome 1 inserted into the region in
176 addition to the *RII_Itera* element. In contrast, in mutant 3BC_3, only the *RII_Itera* element
177 was inserted (**Supplementary Figure S2**, **Extended data**). The *RII_Itera* family of
178 retrotransposons is present in high copy number in the genome of CHE_96224 (107 intact
179 copies with a length of more than 5,000 bp; **Table 2**). We *de-novo* assembled the
180 *AvrPm3*$^{b2/c2}$ region for mutant 3BC_5 and confirmed that the gene coding sequence was
181 disrupted by a *Gypsy* LTR retrotransposon insertion (**Figure 2A, Table 2**, **Supplementary**
182 **Figure S2**). Part of the TE sequence present in the *de-novo* assembly allowed us to assign
183 the TE insertion to a novel TE family (newly named *RLG_Stef*). In contrast to *RII_Itera*,

184 *RLG_Stef* retrotransposons are present in low copy number in CHE_96224 (17 copies with
185 a length of more than 5,000 bp; **Table 2**).
186 For mutant 3BC_6, visual inspection of the genomic mapping file with IGV revealed an
187 irregularity in the sequence of the *AvrPm3*$^{b2/c2}$ promoter region, 1,186 bp before the start
188 of the gene, where a gap in sequence coverage was flanked by reads whose mate reads
189 mapped to a different chromosome, indicating an insertion in this region. Although the
190 *detettore* software did not indicate a TE insertion there, this pattern was highly similar to
191 the TE insertions of the three 3BC insertion mutants. Thus, we de-novo assembled the
192 *AvrPm3*$^{b2/c2}$ region for mutant 3BC_6 and detected an insertion of a TE belonging to a
193 previously uncharacterized family of *Copia* LTR retrotransposons (newly named *RLC_Lily*)
194 (**Supplementary Figure S2**). We observed that RLC_Lily retrotransposons are also present
195 in low copy number in CHE_96224 (18 copies; **Table 2**).
196 We performed amplification experiments with long extension times to verify the putative
197 TE insertions. We designed primers to amplify the putative insertions in mutants 3BC_3
198 and 3BC_4 (Mix_3BC3/4), 3BC_5 (Mix_3BC5), and 3BC_6 (Mix_3BC6). As a control, part of
199 the *AvrPm3*$^{b2/c2}$ gene was amplified (Mix_Avr; **Figure 2B**). As expected, no amplification in
200 the large deletion mutant 3BC_2 occurred with any of the primer mixes, and fragments of
201 the expected size were only amplified for CHE_96224 and the point mutation mutant
202 3BC_1. For the other 3BC mutants, the amplicon size was larger than expected in all
203 putative TE insertion sites, confirming the insertion of foreign DNA in the range of more
204 than 5,000 bp (**Figure 2B**), which is consistent with the average size of a full-length TE of

205 the detected TE families (**Table 2**). No amplification was observed with Mix_3BC6 in
206 mutant 3BC_6, suggesting that insertion size may be larger than in the other mutants.
207 Alternatively, the PCR conditions used were unsuitable for proper amplification of this
208 newly identified TE. We further analyzed the impact of the TE insertions on gene
209 expression. We observed a significant reduction in *AvrPm3*$^{b2/c2}$ expression levels in all 3BC
210 mutants: more than 3-fold in 3BC_1 to up to 90-fold in 3BC_4 (**Figure 2C**). We concluded
211 that modifications of *AvrPm3*$^{b2/c2}$ of different types, i.e., point mutations, deletions or TE
212 insertions causing reduced gene expression and gene disruption, can all lead to loss of
213 recognition by both *Pm3b* and *Pm3c*.
214
215 <u>Gain of virulence on *Pm3f* does not cause virulence on the companion *R* gene *Pm3a*</u>
216 We then set out to identify *Bgt* mutants with gain of virulence on *Pm3f* and *Pm3a*. We
217 found two *Bgt* mutants with gain of virulence on *Pm3f* (hereafter referred to as 3F
218 mutants), and both remained avirulent on *Pm3a* (**Supplementary Figure S3**), although
219 the two *R* genes have an overlapping resistance spectrum. This finding supported the
220 hypothesis that in addition to the commonly recognized AvrPm3$^{a2/f2}$, a second Avr is
221 recognized by Pm3a, but not by Pm3f (Bourras et al. 2015). Mutant 3F_1 had a 107kb
222 deletion in the *AvrPm3*$^{a2/f2}$ locus, resulting in the loss of the two *AvrPm3*$^{a2/f2}$ copies and
223 four additional genes (**Supplementary Table S4**), thus explaining the gain of virulence on
224 *Pm3f*. Interestingly, mutant 3F_2 had a single SNP in the coding region of *AvrPm3*$^{a2/f2}$ in
225 about 50% of the reads (F95Y). Visual inspection of the genomic mapping file of mutant

226 3F_2 was necessary to discover this point mutation, as the filtering criteria used for the
227 SNP call were too stringent, requiring the variant to be present in at least 70% of the reads
228 to be considered a SNP. Previous studies have shown that CHE_96224 has two copies of
229 *AvrPm3*$^{a2/f2}$ based on examination of sequencing coverage (Müller et al. 2019). However,
230 distinguishing the two copies at the genome level is not possible with the available
231 assembly. We therefore hypothesized that in mutant 3F_2 one of the *AvrPm3*$^{a2/f2}$ copies is
232 intact, while the other is mutated. McNally et al. (2018) found natural *Bgt* isolates with a
233 single point mutation at the same position (F95L) and defined it as a virulent allele, since
234 all isolates with this mutation were virulent on *Pm3f*. Although the natural mutation is
235 different from the one present in mutant 3F_2, our data support the hypothesis that a
236 single SNP in position 95 confers virulence, implying that this position is critical for the
237 recognition of AvrPm3$^{a2/f2}$ by Pm3f. Furthermore, the fact that in mutant 3F_2 one copy of
238 *AvrPm3*$^{a2/f2}$ is still intact, while the other has a point mutation, indicates that one mutated
239 gene copy is sufficient to disrupt recognition. As the two mutants on *Pm3f* were still
240 avirulent on *Pm3a*, we concluded that loss or mutation of *AvrPm3*$^{a2/f2}$ results in disrupted
241 recognition by Pm3f, but it is not sufficient to avoid recognition by the broader resistance
242 allele *Pm3a*.

243

244 <u>The *Pm3a* gain-of-virulence mutants show additional virulence on a tandem kinase *R* gene</u>

245 The fact that gain of virulence on *Pm3f* does not lead to virulence on *Pm3a* suggests that
246 Pm3f specifically recognizes AvrPm3$^{a2/f2}$, whereas Pm3a can recognize AvrPm3$^{a2/f2}$,as well

247 as an additional Avr component, hereafter defined as AvrPm3^{a3}, for consistency with
248 previous nomenclature (Bourras et al. 2015). To identify *AvrPm3^{a3}*, we used the large
249 deletion mutant 3F_1 as a parental isolate for a secondary UV mutagenesis to ultimately
250 obtain mutants with gain of virulence on both *Pm3f* and *Pm3a* (3F+A mutants). We
251 identified six 3F+A mutants that were fully virulent on *Pm3a* and *Pm3f*. We wanted to
252 investigate whether the gain of virulence of the 3F+A mutants on *Pm3a* was specific or
253 whether avirulence on other *Pm* genes was also compromised. Accordingly, we performed
254 phenotyping on different wheat NILs containing the resistance genes *Pm1a*, *Pm2*, *Pm3b*,
255 *Pm3c*, *Pm3d*, *Pm3e*, *Pm4a*, *Pm4b*, *Pm8* and *Pm24*, the wheat 1AL.1RS translocation line
256 "Amigo", containing *Pm17*, and four *Aegilops tauschii* lines containing *WTK4*. All six 3F+A
257 mutants remained avirulent on the *Pm* genes encoding NLRs, indicating that NLR-based
258 immunity and recognition was specifically compromised only for *Pm3a* (**Figure 3**,
259 **Supplementary Figure S4**). Avirulence to the chimeric MCTP-kinase proteins Pm4a and
260 Pm4b, and to the tandem kinase protein Pm24 was also not affected. Surprisingly, all six
261 3F+A mutants, besides being virulent on *Pm3f* and *Pm3a*, showed a gain of virulence on
262 the *Ae. tauschii* accessions carrying the tandem kinase resistance gene *WTK4* (**Figure 3**,
263 **Supplementary Figure S4**). These data suggest that there is a common pathway
264 specifically controlling avirulence on the NLR *Pm3a* and the tandem kinase immune
265 receptor *WTK4*.
266

267 Sequencing of *Pm3a* virulent mutants reveals mutations in *Bgt-646,* an ankyrin repeat-
268 containing gene conserved across different powdery mildew species

269 We then wanted to determine the genetic cause of the gain of virulence on *Pm3a* and
270 *WTK4*. Whole genome sequencing and mutation overlap analysis revealed that three
271 independent 3F+A mutants, 3F+A_1, 3F+A_2 and 3F+A_3, had mutations in the *Bgt-646*
272 gene (**Figure 4**). In addition, 3F+A_4 had a SNP 2.7 kb upstream of *Bgt-646* which,
273 however, did not affect its expression (**Supplementary Figure S5**), and, therefore, it is
274 unclear whether this mutation is causative for virulence on *Pm3a*. Mutants 3F+A_4, 3F+A_5
275 and 3F+A_6 did not have other commonly mutated genes (**Supplementary Table S4**).
276 None of the 3F+A mutants had reduced *Bgt-646* expression compared to the parental
277 isolate 3F_1 (**Supplementary Figure S5**). Since at least three of the 3F+A mutants have
278 *Bgt-646* mutated, and no other common mutation was found, we conclude that this gene
279 plays a role in avirulence to *Pm3a*, and also *WTK4*.

280 *Bgt-646* encodes a nuclear protein with a length of 939 amino acids, containing two
281 ankyrin repeat domains of 42 and 92 amino acids (**Figure 4, Supplementary Figure S6**).
282 Because no signal peptide is predicted and the protein is relatively large, *Bgt-646* differs
283 considerably from previously described *Bgt* avirulence components, which are mostly
284 small, secreted effector proteins (Praz et al. 2017; Bourras et al. 2016, 2015, 2019; McNally
285 et al. 2018). We examined the allelic diversity of *Bgt-646* using 102 representative isolates
286 from a global collection of 172 wheat powdery mildew isolates (Sotiropoulos et al. 2022),
287 and found that the gene is highly conserved, with only one isolate having a non-

288 synonymous SNP at position 376 (K376M). We also included 14 isolates collected on the
289 host plants *Triticum dicoccum* or *Triticum turgidum* subsp. *durum* and found among them
290 eight isolates with a non-synonymous SNP at position 4 (P4S) and one SNP in the intron
291 (**Supplementary Table S5**). A single homolog of *Bgt-646* was found in *Blumeria graminis*
292 f. sp. *triticale,* whereas two homologs were identified in *B. g.* f. sp. *hordei* (100, 97 and 97%
293 protein sequence identity, respectively; **Figure 5**, **Supplementary Figure S7**). In addition
294 to the homologs in cereal powdery mildews, we identified eight proteins with >70% amino
295 acid sequence identity to Bgt-646, all from different powdery mildew species: four from
296 *Golovinomyces* sp., three from *Erysiphe* sp. and one from *Podosphaera aphanis*, none of
297 which have been functionally studied (**Figure 5**, **Supplementary Figure S7**). To better
298 predict a possible function of *Bgt-646*, we searched for homologs in yeast. The closest
299 homolog in yeast is *HOS4*, which is involved in histone deacetylation. However, HOS4
300 shares 30% protein sequence identity with Bgt-646 only in a short region from amino acid
301 793 to 889, corresponding to the second ankyrin repeat domain (**Figure 4**), while the rest
302 of the protein has very low homology. Additionally, we used structural predictions to find
303 structural homologs of Bgt-646. The closest structural homolog of Bgt-646 predicted with
304 high confidence by the Phyre2 software (Kelley et al. 2015) is ANK2_HUMAN, a human
305 ankyrin repeat protein involved in endocytosis and intracellular protein transport.
306 However, a list of more than 100 structural homologs with very high structural homology
307 was generated by Phyre2, possibly because ankyrin repeat proteins are ubiquitous and
308 have highly conserved structures even across different kingdoms despite having multiple

309 functions (Thi et al. 2015). We concluded that these structural predictions may not be
310 informative for Bgt-646 function.
311 We used additional bioinformatic analyses to gain more insight into the protein domain
312 structure of Bgt-646. DNABIND predicted that Bgt-646 is a DNA-binding protein
313 (**Supplementary Table S6**). Further analysis with DP-bind and DRNA-pred also revealed
314 several putative DNA binding sites at the N-terminus, mostly between amino acid residues
315 33 and 47 (**Supplementary Table S7**). Most of the predicted DNA binding sites overlap
316 with a nuclear localization signal (NLS), predicted (with low confidence) by PROSITE and
317 (with high confidence) by WoLF PSORT and LOCALIZER (**Figure 4**, **Supplementary Tables**
318 **S8**, **S9**, **S10**).
319 We concluded that Bgt-646 is a conserved protein in powdery mildews, whose function
320 cannot be inferred based on functionally characterized homologous proteins. Still,
321 predictions suggest that it has a nuclear localization and can bind DNA.
322
323 <u>The gain of virulence on *Pm3a* and *WTK4* is correlated with downregulation of specific</u>
324 <u>effector genes</u>
325 Given that Bgt-646 does not have a predicted signal peptide, it is most likely not exported
326 from the fungus for uptake by plant cells. Moreover, the gain-of-virulence mutants have
327 lost avirulence on the two unrelated *R* genes, *Pm3a* and *WTK4*. These observations
328 suggest that Bgt-646 has a regulatory function in the fungal pathogen rather than
329 interacting (directly or indirectly) with either Pm3a or WTK4 proteins. Thus, based on its

330 predicted nuclear localization and DNA binding sites (**Supplementary Tables S6**, **S7**, **S8**,
331 **S9**, **S10**), we hypothesized that *Bgt-646* might control avirulence by up- or down-
332 regulating the expression of effector genes (e.g., the yet unidentified *AvrPm3*^{a3} and
333 *AvrWTK4*). Accordingly, we tested the expression of five *Bgt* effectors belonging to
334 different effector families (Müller et al. 2019): *AvrPm2, AvrPm3*$^{a2/f2}$, *SvrPm3, AvrPm3*$^{b2/c2}$
335 and *Bgt-55150* (the latter two from the same effector family). Since *AvrPm3*$^{a2/f2}$ is absent
336 in all 3F_1-derived mutants, as expected, none of the mutants showed *AvrPm3*$^{a2/f2}$
337 expression (**Figure 6**). A reduction in *SvrPm3* expression was observed in all 3F+A mutants
338 tested, ranging from 25% to 50% of the expression level in the parental isolate 3F_1
339 (**Figure 6**). Similarly, *Bgt-55150* expression was reduced to 3-20% of the expression level
340 in 3F_1 for all 3F+A mutants tested. In contrast, *AvrPm2* and *AvrPm3*$^{b2/c2}$ expression did
341 not significantly differ from 3F_1 in all 3F+A mutants (**Figure 6**).
342 Thus, the downregulation of effectors appears to be specific, affecting only certain
343 effectors. Even effectors belonging to the same effector family and with high sequence
344 similarity (i.e., *AvrPm3*$^{b2/c2}$ and *Bgt-55150*; Bourras et al. 2019) have differential expression
345 patterns in the 3F+A mutants. We can, therefore, infer that *Bgt-646*, along with the
346 unknown component(s) mutated in the other 3F+A mutants, potentially affects *Bgt*
347 avirulence by controlling the expression of putative *Avr* genes.

348 **Discussion**

349 AvrXpose: a novel tool to identify avirulence determinants in powdery mildew

350 *Avr* genes in cereal powdery mildews have been cloned through map-based cloning,
351 GWAS or by testing a large number of candidate genes in screening approaches (Bourras
352 et al. 2016, 2019). These methods require the sequencing and maintenance of large
353 pathogen populations, which is time-consuming, costly, and arduous for obligate
354 biotrophic pathogens such as *Bgt*. Besides, these methods rely on natural genetic diversity,
355 which restricts the identification of conserved factors. Moreover, since these methods are
356 based on correlation rather than causation, they can be biased, especially when the
357 molecular interactions are more complex than a gene-for-gene interaction. AvrXpose
358 overcomes some of these limitations. This method only necessitates sequencing and
359 maintaining the reference isolate and the derived mutants, and because it is based on
360 causative mutations, it is less biased. Barsoum et al. (2020) already described the potential
361 of UV mutagenesis to induce phenotype-causing mutations in barley powdery mildew. By
362 adding a selection step after mutagenesis (**Figure 1**), we expand the method and make it
363 suitable for forward genetics and functional studies.

364 By identifying 3BC mutants with a gain of virulence on *Pm3b* and *Pm3c*, we confirmed the
365 suitability of AvrXpose for finding *Avrs*. AvrXpose also allowed us to discover that variants
366 causing gain of virulence are not only caused by SNPs or InDels, but also by larger
367 deletions or TE insertions, which can only be uncovered using different and

368 complementary approaches (coverage analysis or TE detection by *detettore;* Stritt and
369 Roulin 2021). For instance, we found that TEs play a role in mildew's escape from
370 recognition, as they were the cause of the gain of virulence in the majority of the 3BC
371 mutants (four out of six). This might be due to the mechanism of AvrPm3$^{b2/c2}$ recognition,
372 which appears to be easily and completely blocked by changes in the *Avr* expression level.
373 For many years, TE activity has been known to be a key player in pathogen evolution,
374 particularly in powdery mildews (Faino et al. 2016; Wicker et al. 2013; Frantzeskakis et al.
375 2018). This was also observed in other pathosystems, for example, in wheat blast, where
376 Inoue et al. (2017) described that the insertion of a retrotransposon upstream of the *Avr*
377 gene *PWT3* caused the wheat blast isolate Br116.5 to gain virulence on *Rwt3*-containing
378 cultivars. The observation that four out of six 3BC mutants are virulent due to TE insertions
379 near *AvrPm3$^{b2/c2}$* is intriguing and further highlights the relevance of TEs in pathogen
380 evolution. What we observe after UV light irradiation might mimic (likely with an increased
381 frequency) what also happens in natural settings, where TE induction often occurs due to
382 environmental stress, and contributes to evolution (Biémont and Vieira 2006). Our results
383 emphasize the importance of considering TE transpositions as phenotype-causing
384 mutations also in mutagenesis screenings.
385 Despite the advantages mentioned, AvrXpose also has some limitations. First, it relies on
386 the quality of TE annotation and consensus sequences (Stritt and Roulin 2021). In the case
387 of *Bgt,* this performed well because TEs are well characterized (Parlange et al. 2011; Wicker
388 et al. 2013). However, this may limit this type of analysis in other organisms with poorer

389 TE annotations or for undescribed TEs. For instance, in the case of mutant 3BC_6, the family
390 of the TE inserted close to *AvrPm3*$^{b2/c2}$ was not known, and only the fact that we already
391 knew the *Avr* locus allowed us to find the mutation (**Table 2**). Ideally, this issue could be
392 circumvented by conducting a global analysis to identify the differentially expressed
393 gene(s) in a specific mutant. Second, our mutant screen is far from saturation, potentially
394 limiting our ability to detect additional genetic components controlling avirulence. For
395 example, we did not find commonly mutated genes in at least two of the 3F+A mutants
396 despite using different approaches. Regarding mutant 3F+A_4, it remains unclear whether
397 the SNP 2.7kb upstream of *Bgt-646* is responsible for its phenotype, as it does not have
398 an impact on *Bgt-646* expression at 48 hours after infection. The mutation may not
399 correlate with the virulence phenotype, for which the actual cause might be analogous to
400 that of mutants 3F+A_5 and 3F+A_6. In any case, our results suggest that there may be
401 more than one powdery mildew gene affecting specific avirulence, and the lack of
402 saturation in our mutagenesis did not allow us to mutate all of them. Nonetheless,
403 generating a larger number of *Bgt* gain-of-virulence mutants or, eventually, performing
404 more rounds of UV mutagenesis to generate more mutations (as done by Barsoum et al.
405 2020) could potentially overcome this limitation and allow to find multiple genetic
406 components governing avirulence.
407
408 <u>The genetic complexity of avirulence differs for highly similar alleles of the *Pm3* immune</u>
409 <u>receptor</u>

410 AvrXpose was straightforward to (re)identify *AvrPm3*$^{b2/c2}$ as the Avr recognized by the
411 Pm3b and Pm3c pair. Interestingly, this was not the case for *Pm3a* and *Pm3f*, although it
412 was found that, like the *Pm3b* and *Pm3c* case, *Pm3a* has overlapping, but broader
413 resistance than *Pm3f*. Indeed, the 3F mutants were not virulent on *Pm3a*. Interestingly,
414 despite belonging to the same *Pm3* allelic series, we never identified a gain-of-virulence
415 mutant on *Pm3d* or *Pm3e*. Bourras et al. (2015) suggested that, similar to *Pm3a*, avirulence
416 on *Pm3d* is determined by three distinct genetic components in the pathogen, among
417 which the suppressor *SvrPm3* and the canonical effector *AvrPm3d* have been identified
418 (Bourras et al. 2019). The fact that we did not find *Pm3d*-virulent mutants supports the
419 hypothesis that Pm3d can recognize two Avrs, similar to what was observed also for Pm1a
420 (Kloppe et al. 2023). The case of *Pm3e* may also be similar to *Pm3d*, as *Pm3e* differs by
421 only three point mutations from *Pm3d* (Yahiaoui, Brunner, and Keller 2006). Identifying
422 avirulence components could be further complicated if they were multicopy genes. This
423 may be the case for *AvrPm3*^{a3} as well.
424 We conclude that the *Pm3-AvrPm3* system is much more complex than a single gene-for-
425 gene interaction, and further investigation is needed to unravel all the components
426 involved from the pathogen side. Nevertheless, AvrXpose expands our knowledge of the
427 *Pm3-AvrPm3* system by unraveling the genetics behind *Pm3* allelic specificity and
428 recognition of different *Avr* components by clarifying the effect of specific mutations in
429 some *Avrs* on *Pm3* race-specific avirulence.
430

431 *Bgt-646* is a novel, specific regulator of avirulence

432 Three independent mutants carrying mutations in *Bgt-646* were virulent on both *Pm3a*
433 and *WTK4*. We confirmed the specificity of that gain of virulence by phenotyping several
434 *Pm* gene-containing lines, which remained resistant, confirming that *Bgt-646* plays a role
435 in regulating avirulence specifically on *Pm3a* and *WTK4*. Notably, avirulence to *Pm24*, a
436 tandem kinase *R* gene like *WTK4* (Lu et al. 2020), was also not affected in these mutants.
437 It seems unlikely that *Bgt-646* encodes for the effector recognized by Pm3a or WTK4 due
438 to its large size, the absence of a RNAse-like fold structure, and the lack of a predicted
439 signal peptide. The putative DNA binding capacity, the predicted nuclear localization, and
440 the expression downregulation of specific *Bgt* effectors led us to hypothesize that *Bgt-646*
441 controls race-specific avirulence in *Bgt* by influencing putative *Avr* gene expression (**Figure**
442 **7**). Experimental evidence showing subcellular localization and DNA binding capacity of
443 Bgt-646 could further clarify its role in expression regulation. Additional 3F+A mutants
444 with intact *Bgt-646* indicate that, in addition to *Bgt-646*, there are one or more additional
445 components (shown as CoF6 in **Figure 7**) controlling avirulence specifically on both the
446 *Pm3a* and *WTK4 R* genes. Interestingly, regardless of the presence of an intact *Bgt-646*, all
447 3F+A mutants tested showed the same effector downregulation pattern, which is another
448 indication that both *Bgt-646* and the unidentified component(s) (e.g. *CoF6*) contribute to
449 the same regulatory mechanism, which argues against the unidentified component(s)
450 being the recognized effector(s). Moreover, if *Bgt-646* and the unidentified component
451 had the same function, we would not observe virulence when only one was mutated due

452 to redundancy. Therefore, they may be part of a higher-order regulatory complex, and
453 both are required to regulate the expression of specific effectors. If either of them was
454 mutated, the result would be a loss of avirulence (**Figure 7**).
455 However, the mechanisms by which *Bgt-646* affects expression remain unclear. It has been
456 previously described that knockout of a regulatory gene can affect the expression of
457 effector genes. For example, *Sge1* is a known transcriptional regulator that specifically
458 downregulates effector expression in different pathogenic fungi (Santhanam and Thomma
459 2013; Michielse et al. 2009). On the other side, ankyrin repeat-containing proteins playing
460 a role in pathogenesis have been described, such as RARP-1, a periplasmic protein that
461 supports infection of the bacterial pathogen *Rickettsia parkeri* (Sanderlin, Hanna, and
462 Lamason 2022). Ankyrin repeat proteins have often been shown to have transcriptional
463 functions, at least in plants (Thi et al. 2015). In fungi, a well-studied group of proteins with
464 transcriptional regulatory functions are the APSES family proteins, which have DNA-
465 binding domains and additional domains, often ankyrin repeats (Zhao et al. 2015).
466 Although *Bgt-646* does not have the conserved DNA-binding domain of the APSES family,
467 the prediction of DNA-binding sites in *Bgt-646* may indicate a similar expression-
468 controlling function.
469 A chromosome-scale assembly of the 3F+A mutants could reveal whether there are
470 additional mutated genes that we have not found with AvrXpose. Furthermore, a
471 transcriptomic experiment comparing gene expression of the 3F+A mutants with their

472 avirulent parent would unravel the complete set of differentially regulated effectors, and
473 thus also support the identification of the still unknown *AvrPm3*^{a3} and *AvrWTK4*.
474 This study aimed to develop a method for finding *Avrs* and unraveling additional genetic
475 components involved in avirulence on different *Pm3* alleles. We demonstrated the
476 potential of AvrXpose to discover *Avr* effectors, as well as a conserved regulatory factor
477 (i.e. *Bgt-646*) and showed that this methodology also allows to unravel the different
478 mechanisms of recognition evasion in different *Avr-R* systems.

480 **Materials and Methods**

481 Plant and fungal material

482 Wheat cultivars Kanzler (accession number K-57220) and Chancellor (accession number K-
483 51404) were used as mildew susceptible controls and to maintain the powdery mildew
484 isolates. Near isogenic lines (NILs) Asosan/8*Chancellor, Chul/8*Chancellor,
485 Sonora/8*Chancellor, Kolibri, W150 and Michigan Amber/8*Chancellor (described by
486 Brunner et al. 2010) were used to test for *Pm3a*-, *Pm3b*-, *Pm3c*-, *Pm3d*-, *Pm3e* and *Pm3f*-
487 mediated resistance, respectively. The transgenic line E#2 was used to assess *Pm3e*-
488 mediated resistance (Koller et al. 2018). To test the virulence specificity of the mutant
489 wheat mildew isolates, the wheat NILs Axminster/8*Chancellor, containing *Pm1a*
490 (described by Hewitt et al. 2020), Federation*4/Ulka, containing *Pm2* (Sánchez-Martín et
491 al. 2016), Khapli/8*Chancellor//8*Federation, containing *Pm4a*, Federation*8/W804,
492 containing *Pm4b* (described by Sánchez-Martín et al. 2021), Kavkaz/4*Federation,
493 containing *Pm8* (Hurni et al. 2013), USDA_Pm24 containing Pm24 and the 1AL.1RS
494 translocation line "Amigo", containing *Pm17* (described by Müller et al. 2022), were used.
495 *Aegilops tauschii* accessions from a diversity panel (e.g. TOWWC063, TOWWC087,
496 TOWWC112 and TOWWC154; Arora et al. 2019) containing the resistance gene *WTK4*
497 were used to assess powdery mildew virulence on *WTK4*.

498 *Blumeria graminis* f. sp. *tritici* (*Bgt*) isolate CHE_96224 (Müller et al. 2019) and the derived
499 *Bgt* mutants were used for phenotyping experiments to evaluate gain-of-virulence

500 phenotypes. CHE_96224 is avirulent (no visible disease symptoms observed) on all
501 previously mentioned *R* gene containing wheat and *Ae. tauschii* accessions, except for the
502 *Pm1a* and *Pm8* containing lines, while all the *Bgt* mutants show virulence on one or more
503 of the previously described wheat lines.

504 Mutagenesis and phenotyping experiments

505 Plants used for mutagenesis and phenotyping experiments were grown (16 h light, 8 h
506 dark, 18°C and 60% humidity) for 9-12 days in the case of wheat and 12-17 days for *Ae.*
507 *tauschii* lines. Leaves were then cut into 3 cm fragments and placed in Petri dishes
508 containing water agar supplemented with benzimidazole (5 ppm, MERCK, 51-17-2). They
509 were then spray-inoculated with *Bgt* isolates as described by Hurni et al. (2013). At least
510 three biological replicates were used per inoculation.

511 For mutagenesis, *Bgt* isolates CHE_96224 or 3F_1 were grown on the susceptible wheat
512 line Kanzler for 7 days, irradiated with UV-C light in a UV cabinet (Herolab Crosslinker CL-1,
513 254nm version) as described by Barsoum et al. (2020) and directly used for inoculation of
514 9-12 days old Kanzler leaf segments placed on Petri dishes as described above (**Figure 1**).
515 The irradiation time varied between 2 and 10 min and was adjusted to the time at which
516 50% leaf coverage by powdery mildew was achieved (usually between 4-6 min). For
517 example, if survival was too low after the first irradiation step (e.g., <20% coverage), we
518 irradiated for 2 min in the second step. Conversely, if survival was too high (>80% leaf
519 coverage), we increased the irradiation time to 10 min in the second step. This procedure

520 was repeated twice, resulting in three total rounds of UV irradiation. Finally, the irradiated
521 spore mixture was used to inoculate wheat or *Ae. tauschii* lines containing different *R*
522 genes. *Bgt* colonies growing on the resistant lines were propagated on freshly cut Kanzler
523 leaves placed on agar Petri dishes. After four days, leaf segments containing single
524 colonies were cut and transferred to a new Petri dish. This isolation procedure was
525 repeated twice to ensure genetic homogeneity of the isolated *Bgt* mutants. After obtaining
526 sufficient spores, the phenotype of the selected mutants was evaluated on a diverse panel
527 of wheat and *Ae. tauschii* lines containing different *Pm* genes to confirm their virulence
528 spectrum, and spores were collected for DNA extraction and subsequent sequencing.
529 Disease levels were assessed by eye 7-8 days after inoculation and the virulence was based
530 on the percentage of the leaf area covered by the fungal mycelia (avirulent: <25%, virulent:
531 >25% leaf coverage).

532 <u>DNA extraction and whole genome sequencing</u>

533 DNA extraction using a chloroform and CTAB-based protocol was performed as described
534 by Bourras et al. (2015). Library preparation and Illumina whole genome sequencing were
535 performed at the Functional Genomics Center (Zurich, Switzerland) and Novogene
536 (Cambridge, United Kingdom) using the NovaSeq 6000 technology. Paired-end sequence
537 reads of 150 base pairs (bp) and an insert size of approximately 350 bp generated 1.5 to
538 13 Gb of sequence data per *Bgt* isolate, resulting in an average genome coverage of 25x
539 to 150x. The other *Bgt* isolates described in this study were previously sequenced using

540 the same technology and DNA extraction protocol. Sequences of CHE_96224 and the
541 isolates used to examine *Bgt-646* haplotype diversity (**Supplementary Table S5**) are
542 available at NCBI (Sotiropoulos et al. 2022; McNally et al. 2018).

543 Trimming, mapping, variant calling and transposable element detection

544 To prepare the Illumina reads for subsequent analysis, we trimmed and mapped the reads
545 as described in Sotiropoulos et al. (2022). Briefly, the obtained raw reads were first trimmed
546 for contamination from the Illumina oligo adapter and the sequence quality was checked
547 using Trimmomatic v. 0.39 (Bolger, Lohse, and Usadel 2014). The trimmed reads were then
548 mapped to the reference genome of the *Bgt* isolate CHE_96224, version 3.16 (Müller et al.
549 2019) using bwa mem v0.7 (Li and Durbin 2009). Finally, Samtools v1.9 (Li et al. 2009) was
550 used to sort and remove duplicates to subsequently generate and index the mapping
551 (bam) files used for haplotype calling. Mapping quality and coverage were visually
552 inspected using the integrative genomics viewer IGV (Robinson et al. 2011).

553 Haplotype calling was performed with Freebayes (Garrison and Marth 2012), applying the
554 parameters -p 1 -m 30 -q 20 -z 0.03 -F 0.7 -3 200 as described in Müller et al. (2019). Single
555 nucleotide polymorphisms (SNPs) and insertions/deletions (InDels) were then filtered
556 using Vcftools to obtain variants with less than 10% missing data (Danecek et al. 2011).
557 The resulting vcf file was transformed into hapmap format using Tassel5 (Bradbury et al.
558 2007). TE insertions were detected using the software *detettore*, with default parameters
559 (Stritt and Roulin 2021). Coverage analysis to detect possibly deleted or duplicated genes

560 was performed using an in-house Python script (retrievable from
561 https://gist.github.com/caldetas/24576da33d1ff91057ecabb1c5a3b6af). The annotation
562 version 4.20 of CHE_96224 was used to select variants less than 1.5 or 2 kb away (for SNPs
563 and TE insertions, respectively) from annotated genes. To avoid overlooking variants, we
564 also checked whether we found variants in one mutant close to variants in other mutants.
565 Only variants uniquely occurring in a mutant were retained for further analyses
566 (**Supplementary Tables S1**, **S2**, **S3**). All variants close to annotated genes were then
567 visually inspected and confirmed using IGV.

568 *Bgt-646* domains and motifs predictions

569 A variety of software programs were used to predict the protein domains and properties
570 of *Bgt-646*. DNABIND, DP-bind and DRNA-pred were used to predict DNA binding
571 residues (Hwang, Gou, and Kuznetsov 2007; Szilagyi and Skolnick 2006; Yan and Kurgan
572 2017). ScanPROSITE, LOCALIZER and WoLF PSORT were used to predict domains and
573 subcellular localization (https://prosite.expasy.org/; Sperschneider et al. 2017; Horton et
574 al. 2007). Details and prediction results are described in **Supplementary Tables S6, S7,**
575 **S8, S9** and **S10**.

576 Multiple sequence alignment and phylogenetic tree of *Bgt-646* homologs

577 Homologs of Bgt-646 were searched in the NCBI database using Protein Blast with default
578 parameters (https://blast.ncbi.nlm.nih.gov). A multiple sequence alignment was
579 performed using COBALT (Papadopoulos and Agarwala 2007), available directly from the

580 NCBI website. COBALT uses information from conserved domain and protein motif
581 databases, and sequence similarity based on RPS-BLAST, BLASTP, and PHI-BLAST. The
582 multiple alignment is shown in **Supplementary Figure S7**. A phylogenetic tree was
583 constructed using FastTree (Price, Dehal, and Arkin 2009), visualized and modified using
584 FigTree v1.4.4 (retrievable from https://github.com/rambaut/figtree/releases/tag/v1.4.4).
585 The Phyre2 web portal was used to predict structural homologs (Kelley et al. 2015).

586 PCR, qPCR experiments and statistical analyses

587 PCRs for amplification of transposable element insertions were performed using Phusion®
588 High-Fidelity DNA Polymerase (M0530S, New England BioLabs Inc.) according to the
589 manufacturer's recommendations, with an annealing temperature of 59 °C and an
590 extension time of 3 min.

591 To study the expression of specific genes, RT-qPCR experiments were performed
592 according to the MIQE guidelines (Bustin et al. 2009). mRNA samples were extracted from
593 infected leaf material obtained from three to five independent biological replicates 2 days
594 after *Bgt* infection, using the Dynabeads mRNA DIRECT Kit (Invitrogen). cDNA was then
595 synthesized using the Maxima H Minus First Strand cDNA Synthesis Kit (ThermoFisher),
596 according to the manufacturer. Fungal glyceraldehyde 3-phosphate dehydrogenase
597 ($GAPDH_{Bgt}$) was used as an internal control to normalize gene expression. The KAPA SYBR
598 FAST qPCR kit (Kapa Biosystems) was used to amplify the gene of interest and the internal
599 control in a CFX384 Touch Real-Time PCR Detection System (Bio-Rad). Gene expression

600 was analyzed with the CFX Maestro software version 3.1 (Bio-Rad). To assess statistical
601 differences between groups an analysis of variance (ANOVA) was performed, followed by
602 a Tukey HSD test. The analyses were performed in R using the functions *aov* and
603 *TukeyHSD*, respectively. Letters corresponding to significance groups have been assigned
604 using *glht* and *cld* functions of the *multcomp* package (Bretz, Hothorn, and Westfall 2010).
605 The results of the statistical analyses are described in **Supplementary Table S11**.

606 PCR and RT-qPCR primers for promoter regions, reference, and target genes of *Bgt* are
607 listed in **Supplementary Table S12**.

608 Data availability

609 Raw fasta sequences of all *Bgt* mutants generated in this study are available through
610 NCBI (BioProject ID: PRJNA1016363).

Acknowledgements

We thank Gerhard Herren and Victoria Widrig for the help with RT-qPCR and for technical support, Dr. Lukas Kunz and Dr. Marion C. Müller for fruitful discussions and material, and the Functional Genomics Center Zurich of the University of Zurich (FCGZ) for sequencing. We also thank Prof. Dr. Christina Cowger, Small Grains Pathologist, USDA-ARS, Department of Plant Pathology, North Carolina State University for providing us with the *Pm24* differential line.

Funding

This work was supported by the Swiss National Science Foundation grants 310030B_182833 and 310030_204165. JSM is recipient of the grant 'Ramon y Cajal' Fellowship RYC2021-032699-I funded by MCIN/AEI/10.13039/501100011033.

Author Contributions

ZB, JSM and BK conceived the experiments, interpreted results, and wrote the manuscript. ZB and US produced the *Bgt* mutants and performed the phenotyping experiments. US performed the RT-qPCR experiments. ZB, TW, AGS, JG and MH contributed to the bioinformatic analyses. All authors have read and agreed to the published version of the manuscript.

Conflict of Interest Statement

629 The authors declare no conflict of interest.

630 **Literature Cited**

631 Arora, Sanu, Burkhard Steuernagel, Kumar Gaurav, Sutha Chandramohan, Yunming Long,
632 Oadi Matny, Ryan Johnson, et al. 2019. "Resistance Gene Cloning from a Wild Crop
633 Relative by Sequence Capture and Association Genetics." *Nature Biotechnology* 37
634 (2): 139–43. https://doi.org/10.1038/s41587-018-0007-9.

635 Barsoum, Mirna, Stefan Kusch, Lamprinos Frantzeskakis, Ulrich Schaffrath, and Ralph
636 Panstruga. 2020. "Ultraviolet Mutagenesis Coupled with Next-Generation
637 Sequencing as a Method for Functional Interrogation of Powdery Mildew Genomes."
638 *Molecular Plant-Microbe Interactions* 33 (8): 1008–21. https://doi.org/10.1094/MPMI-
639 02-20-0035-TA.

640 Biémont, Christian, and Cristina Vieira. 2006. "Junk DNA as an Evolutionary Force."
641 *Nature* 443: 521–24. https://doi.org/https://doi.org/10.1038/443521a.

642 Bolger, Anthony M., Marc Lohse, and Bjoern Usadel. 2014. "Trimmomatic: A Flexible
643 Trimmer for Illumina Sequence Data." *Bioinformatics* 30 (15): 2114–20.
644 https://doi.org/10.1093/bioinformatics/btu170.

645 Bourras, Salim, Lukas Kunz, Minfeng Xue, Coraline Rosalie Praz, Marion Claudia Müller,
646 Carol Kälin, Michael Schläfli, et al. 2019. "The AvrPm3-Pm3 Effector-NLR Interactions
647 Control Both Race-Specific Resistance and Host-Specificity of Cereal Mildews on
648 Wheat." *Nature Communications* 10 (2292): 1–16. https://doi.org/10.1038/s41467-
649 019-10274-1.

650 Bourras, Salim, Kaitlin Elyse McNally, Roi Ben-David, Francis Parlange, Stefan Roffler,
651 Coraline Rosalie Praz, Simone Oberhaensli, et al. 2015. "Multiple Avirulence Loci and
652 Allele-Specific Effector Recognition Control the Pm3 Race-Specific Resistance of
653 Wheat to Powdery Mildew." *The Plant Cell* 27: 2991–3012.
654 https://doi.org/10.1105/tpc.15.00171.

655 Bourras, Salim, Kaitlin Elyse McNally, Marion Claudia Müller, Thomas Wicker, and Beat
656 Keller. 2016. "Avirulence Genes in Cereal Powdery Mildews: The Gene-for-Gene
657 Hypothesis 2.0." *Frontiers in Plant Science* 7 (241): 1–7.
658 https://doi.org/10.3389/fpls.2016.00241.

659 Bradbury, Peter J., Zhiwu Zhang, Dallas E. Kroon, Terry M. Casstevens, Yogesh Ramdoss,
660 and Edward S. Buckler. 2007. "TASSEL: Software for Association Mapping of
661 Complex Traits in Diverse Samples." *Bioinformatics* 23 (19): 2633–35.
662 https://doi.org/10.1093/bioinformatics/btm308.

Bretz, Frank, Torsten Hothorn, and Peter Westfall. 2010. *Multiple Comparisons Using R*. *Multiple Comparisons Using R*. 1st editio. Chapman and Hall/CRC. https://doi.org/https://doi.org/10.1201/9781420010909.

Brueggeman, R, N Rostoks, D Kudrna, A Kilian, F Han, J Chen, A Druka, B Steffenson, and A Kleinhofs. 2002. "The Barley Stem Rust-Resistance Gene Rpg1 Is a Novel Disease-Resistance Gene with Homology to Receptor Kinases." *Proceedings of the National Academy of Sciences of the United States of America* 99 (14): 9328–33. https://doi.org/10.1073/pnas.142284999.

Brunner, Susanne, Severine Hurni, Philipp Streckeisen, Gabriele Mayr, Mario Albrecht, Nabila Yahiaoui, and Beat Keller. 2010. "Intragenic Allele Pyramiding Combines Different Specificities of Wheat Pm3 Resistance Alleles." *Plant Journal* 64: 433–45. https://doi.org/10.1111/j.1365-313X.2010.04342.x.

Bustin, Stephen A., Vladimir Benes, Jeremy A. Garson, Jan Hellemans, Jim Huggett, Mikael Kubista, Reinhold Mueller, et al. 2009. "The MIQE Guidelines: Minimum Information for Publication of Quantitative Real-Time PCR Experiments." *Clinical Chemistry* 55 (4): 611–22. https://doi.org/10.1373/clinchem.2008.112797.

Cao, Yu, Florian Kümmel, Elke Logemann, Jan M. Gebauer, Aaron W. Lawson, Dongli Yu, Matthias Uthoff, et al. 2023. "Structural Polymorphisms within a Common Powdery Mildew Effector Scaffold as a Driver of Coevolution with Cereal Immune Receptors." *Proceedings of the National Academy of Sciences of the United States of America* 120 (32): 1–11. https://doi.org/10.1073/PNAS.2307604120.

Chen, Jiapeng, Narayana M. Upadhyaya, Diana Ortiz, Jana Sperschneider, Feng Li, Clement Bouton, Susan Breen, et al. 2017. "Loss of AvrSr50 by Somatic Exchange in Stem Rust Leads to Virulence for Sr50 Resistance in Wheat." *Science* 358 (6370): 1607–10. https://doi.org/10.1126/science.aao4810.

Danecek, Petr, Adam Auton, Goncalo Abecasis, Cornelis A. Albers, Eric Banks, Mark A. DePristo, Robert E. Handsaker, et al. 2011. "The Variant Call Format and VCFtools." *Bioinformatics* 27 (15): 2156–58. https://doi.org/10.1093/bioinformatics/btr330.

Dodds, Peter N., and John P. Rathjen. 2010. "Plant Immunity: Towards an Integrated View of Plant-Pathogen Interactions." *Nature Reviews Genetics* 11: 539–548. https://doi.org/10.1038/nrg2812.

Faino, Luigi, Michael F Seidl, Xiaoqian Shi-Kunne, Marc Pauper, Grardy C M Van Den Berg, Alexander H J Wittenberg, and Bart P H J Thomma. 2016. "Transposons Passively and Actively Contribute to Evolution of the Two-Speed Genome of a Fungal Pathogen." *Genome Research* 26: 1091–1100.

https://doi.org/10.1101/gr.204974.116.

Frantzeskakis, Lamprinos, Barbara Kracher, Stefan Kusch, Makoto Yoshikawa-Maekawa, Saskia Bauer, Carsten Pedersen, Pietro D. Spanu, Takaki Maekawa, Paul Schulze-Lefert, and Ralph Panstruga. 2018. "Signatures of Host Specialization and a Recent Transposable Element Burst in the Dynamic One-Speed Genome of the Fungal Barley Powdery Mildew Pathogen." *BMC Genomics* 19 (381): 1–23. https://doi.org/10.1186/s12864-018-4750-6.

Garrison, Erik, and Gabor Marth. 2012. "Haplotype-Based Variant Detection from Short-Read Sequencing." *ArXiv: Genomics*, 1–9. http://arxiv.org/abs/1207.3907.

Gaurav, Kumar, Sanu Arora, Paula Silva, Javier Sánchez-Martín, Richard Horsnell, Liangliang Gao, Gurcharn S Brar, et al. 2022. "Population Genomic Analysis of Aegilops Tauschii Identifies Targets for Bread Wheat Improvement." *Nature Biotechnology* 40: 422–31. https://doi.org/10.1038/s41587-021-01058-4.

Hewitt, Tim, Marion Claudia Müller, István Molnár, Martin Mascher, Kateřina Holušová, Hana Šimková, Lukas Kunz, et al. 2021. "A Highly Differentiated Region of Wheat Chromosome 7AL Encodes a Pm1a Immune Receptor That Recognizes Its Corresponding AvrPm1a Effector from Blumeria Graminis." *New Phytologist* 229: 2812–26. https://doi.org/10.1111/nph.17075.

Horton, Paul, Keun-Joon Park, Takeshi Obayashi, Naoya Fujita, Hajime Harada, C J Adams-Collier, and Kenta Nakai. 2007. "WoLF PSORT: Protein Localization Predictor." *Nucleic Acids Research* 35: W585–87. https://doi.org/10.1093/nar/gkm259.

Hurni, Severine, Susanne Brunner, Gabriele Buchmann, Gerhard Herren, Tina Jordan, Patricia Krukowski, Thomas Wicker, Nabila Yahiaoui, Rohit Mago, and Beat Keller. 2013. "Rye Pm8 and Wheat Pm3 Are Orthologous Genes and Show Evolutionary Conservation of Resistance Function against Powdery Mildew." *Plant Journal* 76: 957–69. https://doi.org/10.1111/tpj.12345.

Hwang, Seungwoo, Zhenkun Gou, and Igor B Kuznetsov. 2007. "DP-Bind: A Web Server for Sequence-Based Prediction of DNA-Binding Residues in DNA-Binding Proteins." *Bioinformatics* 23 (5): 634–36. https://doi.org/10.1093/bioinformatics/btl672.

Inoue, Yoshihiro, Trinh T.P. Vy, Kentaro Yoshida, Hokuto Asano, Chikako Mitsuoka, Soichiro Asuke, Vu L. Anh, et al. 2017. "Evolution of the Wheat Blast Fungus through Functional Losses in a Host Specificity Determinant." *Science* 357: 80–83. https://doi.org/10.1126/science.aam9654.

732 Jones, Jonathan D. G., and Jeffery L. Dangl. 2006. "The Plant Immune System." *Nature*
733 444: 323–29. https://doi.org/https://doi.org/10.1038/nature05286.

734 Kangara, Ngonidzashe, Tomasz J. Kurowski, Guru V. Radhakrishnan, Sreya Ghosh, Nicola
735 M. Cook, Guotai Yu, Sanu Arora, et al. 2020. "Mutagenesis of Puccinia Graminis f. Sp.
736 Tritici and Selection of Gain-of-Virulence Mutants." *Frontiers in Plant Science* 11: 1–
737 14. https://doi.org/10.3389/fpls.2020.570180.

738 Kelley, Lawrence A, Stefans Mezulis, Christopher M Yates, Mark N Wass, and Michael J E
739 Sternberg. 2015. "The Phyre2 Web Portal for Protein Modeling, Prediction and
740 Analysis." *Nature Protocols* 10 (6): 845–58. https://doi.org/10.1038/nprot.2015.053.

741 Kloppe, Tim, Rebecca B Whetten, Saet-Byul Kim, Oliver R Powell, Stefanie L€ Uck, Dimitar
742 Douchkov, Ross W Whetten, Amanda M Hulse-Kemp, Peter Balint-Kurti, and
743 Christina Cowger. 2023. "Two Pathogen Loci Determine Blumeria Graminis f. Sp.
744 Tritici Virulence to Wheat Resistance Gene Pm1a." *New Phytologist* 238: 1546–61.
745 https://doi.org/10.1111/nph.18809.

746 Klymiuk, Valentyna, Gitta Coaker, Tzion Fahima, and Curtis J Pozniak. 2021. "Tandem
747 Protein Kinases Emerge as New Regulators of Plant Immunity." *Molecular Plant-*
748 *Microbe Interactions* 34 (10): 1094–1102. https://doi.org/10.1094/MPMI-03-21-0073-
749 CR.

750 Koller, Teresa, Susanne Brunner, Gerhard Herren, Javier Sanchez-Martin, Severine Hurni,
751 and Beat Keller. 2018. "Field Grown Transgenic Pm3e Wheat Lines Show Powdery
752 Mildew Resistance and No Fitness Costs Associated with High Transgene
753 Expression." *Transgenic Research* 28: 9–20. https://doi.org/10.1007/s11248-018-
754 0099-5.

755 Li, Heng, and Richard Durbin. 2009. "Fast and Accurate Short Read Alignment with
756 Burrows-Wheeler Transform." *Bioinformatics* 25 (14): 1754–60.
757 https://doi.org/10.1093/bioinformatics/btp324.

758 Li, Heng, Bob Handsaker, Alec Wysoker, Tim Fennell, Jue Ruan, Nils Homer, Gabor Marth,
759 Goncalo Abecasis, and Richard Durbin. 2009. "The Sequence Alignment/Map Format
760 and SAMtools." *Bioinformatics* 25 (16): 2078–79.
761 https://doi.org/10.1093/bioinformatics/btp352.

762 Li, Yuxiang, Meinan Wang, Deven R. See, and Xianming Chen. 2019. "Ethyl-
763 Methanesulfonate Mutagenesis Generated Diverse Isolates of Puccinia Striiformis f.
764 Sp. Tritici, the Wheat Stripe Rust Pathogen." *World Journal of Microbiology and*
765 *Biotechnology* 35 (2): 1–18. https://doi.org/10.1007/s11274-019-2600-6.

766 Lu, Ping, Li Guo, Zhenzhong Wang, Beibei Li, Jing Li, Yahui Li, Dan Qiu, et al. 2020. "A
767 Rare Gain of Function Mutation in a Wheat Tandem Kinase Confers Resistance to
768 Powdery Mildew." *Nature Communications* 11 (680): 1–11.
769 https://doi.org/10.1038/s41467-020-14294-0.

770 Lu, Xunli, Barbara Kracher, Isabel M.L. Saur, Saskia Bauer, Simon R. Ellwood, Roger Wise,
771 Takashi Yaeno, Takaki Maekawa, and Paul Schulze-Lefert. 2016. "Allelic Barley MLA
772 Immune Receptors Recognize Sequence-Unrelated Avirulence Effectors of the
773 Powdery Mildew Pathogen." *Proceedings of the National Academy of Sciences of the*
774 *United States of America* 113 (42): E6486–95.
775 https://doi.org/10.1073/pnas.1612947113.

776 McNally, Kaitlin Elyse, Fabrizio Menardo, Linda Lüthi, Coraline Rosalie Praz, Marion
777 Claudia Müller, Lukas Kunz, Roi Ben-David, et al. 2018. "Distinct Domains of the
778 AVRPM3A2/F2 Avirulence Protein from Wheat Powdery Mildew Are Involved in
779 Immune Receptor Recognition and Putative Effector Function." *New Phytologist* 218:
780 681–95. https://doi.org/10.1111/nph.15026.

781 Michielse, Caroline B., Ringo Van Wijk, Linda Reijnen, Erik M.M. Manders, Sonja Boas,
782 Chantal Olivain, Claude Alabouvette, and Martijn Rep. 2009. "The Nuclear Protein
783 Sge1 of Fusarium Oxysporum Is Required for Parasitic Growth." *PLOS Pathogens* 5
784 (10). https://doi.org/10.1371/JOURNAL.PPAT.1000637.

785 Müller, Marion Claudia, Lukas Kunz, Seraina Schudel, Aaron W. Lawson, Sandrine
786 Kammerecker, Jonatan Isaksson, Michele Wyler, et al. 2022. "Ancient Variation of the
787 AvrPm17 Gene in Powdery Mildew Limits the Effectiveness of the Introgressed Rye
788 Pm17 Resistance Gene in Wheat." *Proceedings of the National Academy of Sciences*
789 *of the United States of America* 119 (30): 1–12.
790 https://doi.org/10.1073/PNAS.2108808119.

791 Müller, Marion Claudia, Coraline Rosalie Praz, Alexandros Georgios Sotiropoulos, Fabrizio
792 Menardo, Lukas Kunz, Seraina Schudel, Simone Oberhaensli, et al. 2019. "A
793 Chromosome-Scale Genome Assembly Reveals a Highly Dynamic Effector
794 Repertoire of Wheat Powdery Mildew." *New Phytologist* 221: 2176–89.
795 https://doi.org/10.1111/nph.15529.

796 Nirmala, Jayaveeramuthu, Tom Drader, Paulraj K. Lawrence, Chuntao Yin, Scot Hulbert,
797 Camille M. Steber, Brian J. Steffenson, Les J. Szabo, Diter Von Wettstein, and Andris
798 Kleinhofs. 2011. "Concerted Action of Two Avirulent Spore Effectors Activates
799 Reaction to Puccinia Graminis 1 (Rpg1)-Mediated Cereal Stem Rust Resistance."
800 *Proceedings of the National Academy of Sciences of the United States of America* 108
801 (35): 14676–81. https://doi.org/10.1073/PNAS.1111771108.

802 Papadopoulos, Jason S, and Richa Agarwala. 2007. "COBALT: Constraint-Based
803 Alignment Tool for Multiple Protein Sequences." *Bioinformatics* 23 (9): 1073–79.
804 https://doi.org/10.1093/bioinformatics/btm076.

805 Parlange, Francis, Simone Oberhaensli, James Breen, Matthias Platzer, Stefan Taudien,
806 Hana Šimková, Thomas Wicker, Jaroslav Doležel, and Beat Keller. 2011. "A Major
807 Invasion of Transposable Elements Accounts for the Large Size of the Blumeria
808 Graminis f.Sp. Tritici Genome." *Functional & Integrative Genomics* 11: 671–77.
809 https://doi.org/10.1007/s10142-011-0240-5.

810 Parlange, Francis, Stefan Roffler, Fabrizio Menardo, Roi Ben-David, Salim Bourras, Kaitlin
811 Elyse McNally, Simone Oberhaensli, et al. 2015. "Genetic and Molecular
812 Characterization of a Locus Involved in Avirulence of Blumeria Graminis f. Sp. Tritici
813 on Wheat Pm3 Resistance Alleles." *Fungal Genetics and Biology* 82: 181–92.
814 https://doi.org/10.1016/j.fgb.2015.06.009.

815 Praz, Coraline R., Salim Bourras, Fansong Zeng, Javier Sánchez-Martín, Fabrizio Menardo,
816 Minfeng Xue, Lijun Yang, et al. 2017. "AvrPm2 Encodes an RNase-like Avirulence
817 Effector Which Is Conserved in the Two Different Specialized Forms of Wheat and
818 Rye Powdery Mildew Fungus." *New Phytologist* 213 (3): 1301–14.
819 https://doi.org/10.1111/nph.14372.

820 Presti, Libera Lo, Daniel Lanver, Gabriel Schweizer, Shigeyuki Tanaka, Liang Liang, Marie
821 Tollot, Alga Zuccaro, Stefanie Reissmann, and Regine Kahmann. 2015. "Fungal
822 Effectors and Plant Susceptibility." *Annual Review of Plant Biology* 66: 513–45.
823 https://doi.org/10.1146/annurev-arplant-043014-114623.

824 Price, Morgan N., Paramvir S. Dehal, and Adam P. Arkin. 2009. "FastTree: Computing
825 Large Minimum Evolution Trees with Profiles Instead of a Distance Matrix."
826 *Molecular Biology and Evolution* 26 (7): 1641–50.
827 https://doi.org/10.1093/MOLBEV/MSP077.

828 Robinson, James T., Helga Thorvaldsdóttir, Wendy Winckler, Mitchell Guttman, Eric S.
829 Lander, Gad Getz, and Jill P. Mesirov. 2011. "Integrative Genomics Viewer." *Nature*
830 *Biotechnology* 29 (1): 24–26. https://doi.org/10.1038/nbt.1754.

831 Salcedo, Andres, William Rutter, Shichen Wang, Alina Akhunova, Stephen Bolus,
832 Shiaoman Chao, Nickolas Anderson, et al. 2017. "Variation in the AvrSr35 Gene
833 Determines Sr35 Resistance against Wheat Stem Rust Race Ug99." *Science* 358
834 (6370): 1604–6. https://doi.org/10.1126/science.aao7294.

835 Sánchez-Martín, Javier, Salim Bourras, and Beat Keller. 2018. "Diseases Affecting Wheat
836 and Barley: Powdery Mildew." In *Integrated Disease Management of Wheat and*

837 *Barley*, 69–93. https://doi.org/10.19103/AS.2018.0039.04.

838 Sánchez-Martín, Javier, and Beat Keller. 2021. "NLR Immune Receptors and Diverse Types
839 of Non-NLR Proteins Control Race-Specific Resistance in Triticeae." *Current Opinion*
840 *in Plant Biology* 62 (August): 1–10. https://doi.org/10.1016/J.PBI.2021.102053.

841 Sánchez-Martín, Javier, Burkhard Steuernagel, Sreya Ghosh, Gerhard Herren, Severine
842 Hurni, Nikolai Adamski, Jan Vrána, et al. 2016. "Rapid Gene Isolation in Barley and
843 Wheat by Mutant Chromosome Sequencing." *Genome Biology* 17 (221): 1–7.
844 https://doi.org/10.1186/s13059-016-1082-1.

845 Sánchez-Martín, Javier, Victoria Widrig, Gerhard Herren, Thomas Wicker, Helen Zbinden,
846 Julien Gronnier, Laurin Spörri, et al. 2021. "Wheat Pm4 Resistance to Powdery
847 Mildew Is Controlled by Alternative Splice Variants Encoding Chimeric Proteins."
848 *Nature Plants* 7 (3): 327–41. https://doi.org/10.1038/s41477-021-00869-2.

849 Sánchez-Vallet, Andrea, Simone Fouché, Isabelle Fudal, Fanny E. Hartmann, Jessica L.
850 Soyer, Aurélien Tellier, and Daniel Croll. 2018. "The Genome Biology of Effector
851 Gene Evolution in Filamentous Plant Pathogens." *Annual Review of Phytopathology*
852 56 (August): 21–40. https://doi.org/10.1146/ANNUREV-PHYTO-080516-035303.

853 Sanderlin, Allen G., Ruth E. Hanna, and Rebecca L. Lamason. 2022. "The Ankyrin Repeat
854 Protein RARP-1 Is a Periplasmic Factor That Supports Rickettsia Parkeri Growth and
855 Host Cell Invasion." *Journal of Bacteriology* 204 (7).
856 https://doi.org/10.1128/JB.00182-22.

857 Santhanam, Parthasarathy, and Bart P.H.J. Thomma. 2013. "Verticillium Dahliae Sge1
858 Differentially Regulates Expression of Candidate Effector Genes." *Molecular Plant-*
859 *Microbe Interactions* 26 (2): 249–56. https://doi.org/10.1094/MPMI-08-12-0198-R.

860 Saur, Isabel ML, Saskia Bauer, Barbara Kracher, Xunli Lu, Lamprinos Franzeskakis, Marion
861 C Mü ller, Bjö rn Sabelleck, et al. 2019. "Multiple Pairs of Allelic MLA Immune
862 Receptor-Powdery Mildew AVR A Effectors Argue for a Direct Recognition
863 Mechanism." *Elife* 8:e44471: 1–31. https://doi.org/10.7554/eLife.44471.001.

864 Sherwood, J. E., B. Slutsky, and S. C. Somerville. 1991. "Induced Morphological and
865 Virulence Variants of the Obligate Barley Pathogen Erysiphe Graminis f. Sp. Hordei."
866 *Phytopathology* 81 (11): 1350–57. https://doi.org/10.1094/phyto-81-1350.

867 Sotiropoulos, Alexandros G., Epifanía Arango-Isaza, Tomohiro Ban, Chiara Barbieri, Salim
868 Bourras, Christina Cowger, Paweł C. Czembor, et al. 2022. "Global Genomic Analyses
869 of Wheat Powdery Mildew Reveal Association of Pathogen Spread with Historical
870 Human Migration and Trade." *Nature Communications* 13 (1): 1–14.

871 https://doi.org/10.1038/s41467-022-31975-0.

872 Sperschneider, Jana, Ann-Maree Catanzariti, Kathleen Deboer, Benjamin Petre, Donald M
873 Gardiner, Karam B Singh, Peter N Dodds, and Jennifer M Taylor. 2017. "LOCALIZER:
874 Subcellular Localization Prediction of Both Plant and Effector Proteins in the Plant
875 Cell." *Scientific Reports* 7. https://doi.org/10.1038/srep44598.

876 Stirnweis, Daniel, Samira Désiré Milani, Tina Jordan, Beat Keller, and Susanne Brunner.
877 2014. "Substitutions of Two Amino Acids in the Nucleotide-Binding Site Domain of a
878 Resistance Protein Enhance the Hypersensitive Response and Enlarge the PM3F
879 Resistance Spectrum in Wheat." *MPMI* 27 (3): 265–76.
880 https://doi.org/10.1094/MPMI-10-13-0297-FI.

881 Stritt, Christoph, and Anne C. Roulin. 2021. "Detecting Signatures of TE Polymorphisms in
882 Short-Read Sequencing Data." In *Plant Transposable Elements: Methods and*
883 *Protocols*, 2250:177–87. Springer Nature. https://doi.org/10.1007/978-1-0716-1134-
884 0_17.

885 Szilagyi, András, and Jeffrey Skolnick. 2006. "Efficient Prediction of Nucleic Acid Binding
886 Function from Low-Resolution Protein Structures." *Journal of Molecular Biology* 358
887 (3): 922–33. https://doi.org/10.1016/j.jmb.2006.02.053.

888 Takamatsu, Susumo. 2004. "Phylogeny and Evolution of the Powdery Mildew Fungi
889 (Erysiphales, Ascomycota) Inferred from Nuclear Ribosomal DNA Sequences."
890 *Mycoscience* 45 (2): 147–57. https://doi.org/10.1007/S10267-003-0159-3.

891 Thi, Kieu, Xuan Vo, Chi-Yeol Kim, Anil Kumar, Nalini Chandran, Ki-Hong Jung, Gynheung
892 An, and Jong-Seong Jeon. 2015. "Molecular Insights into the Function of Ankyrin
893 Proteins in Plants." *J. Plant Biol* 58: 271–84. https://doi.org/10.1007/s12374-015-
894 0228-0.

895 Upadhyaya, Narayana M., Rohit Mago, Vinay Panwar, Tim Hewitt, Ming Luo, Jian Chen,
896 Jana Sperschneider, et al. 2021. "Genomics Accelerated Isolation of a New Stem Rust
897 Avirulence Gene–Wheat Resistance Gene Pair." *Nature Plants* 7 (9): 1220–28.
898 https://doi.org/10.1038/s41477-021-00971-5.

899 Wicker, Thomas, Simone Oberhaensli, Francis Parlange, Jan P Buchmann, Margarita
900 Shatalina, Stefan Roffler, Roi Ben-David, et al. 2013. "The Wheat Powdery Mildew
901 Genome Shows the Unique Evolution of an Obligate Biotroph." *Nature Genetics* 45
902 (9): 1092–96. https://doi.org/10.1038/ng.2704.

903 Yahiaoui, Nabila, Susanne Brunner, and Beat Keller. 2006. "Rapid Generation of New
904 Powdery Mildew Resistance Genes after Wheat Domestication." *Plant Journal* 47:

905 85–98. https://doi.org/10.1111/j.1365-313X.2006.02772.x.

906 Yan, Jing, and Lukasz Kurgan. 2017. "DRNApred, Fast Sequence-Based Method That
907 Accurately Predicts and Discriminates DNA-and RNA-Binding Residues." *Nucleic*
908 *Acids Research* 45 (10): 1–16. https://doi.org/10.1093/nar/gkx059.

909 Zhao, Yong, Hao Su, Jing Zhou, Huihua Feng, Ke-Qin Zhang, and Jinkui Yang. 2015. "The
910 APSES Family Proteins in Fungi: Characterizations, Evolution and Functions." *Fungal*
911 *Genetics and Biology* 81: 271–80. https://doi.org/10.1016/j.fgb.2014.12.003.

Tables

Table 1. Number and types of sequence variants present in the 3BC, 3F and 3F+A *Bgt* mutants.

Parental isolate	CHE_96224								3F_1					
Mutant group	**3BC**						**3F**		**3F+A**					
Mutant name	3BC_1	3BC_2	3BC_3	3BC_4	3BC_5	3BC_6	3F_1	3F_2	3F+A_1	3F+A_2	3F+A_3	3F+A_4	3F+A_5	3F+A_6
SNPs – whole genome [a]	582	253	572	321	267	381	973	640	831	754	899	975	822	822
Unique SNPs [b]	125	84	125	62	67	58	508	234	89	116	90	98	78	41
Gene-proximal variants (GPV) - **Total** [c]	23	7	5	9	3	6	13	26	8	24	8	14	10	4
GPV - SNPs	22	5	4	3	2	2	7	26	8	20	8	13	6	2
GPV - Copy number variations	-	1	-	-	-	-	5	-	-	-	-	-	-	-
GPV -TE insertions	1	1	1	6	1	4	1	-	-	4	-	1	4	2

[a] Total number of SNPs compared with the parental isolate (CHE_96224 or 3F_1) detected by Freebayes and filtered with quality criteria as described in Materials & Methods. In this category are also included small insertions or deletions (max. 7bp), which can be detected with Freebayes. Bigger deletions are listed in the category "Copy number variations".

[b] Number of unique SNPs, e.g. SNPs only present in one isolate and not in any other isolate of the same mutant group (**Supplementary Tables S1, S2, S3**).

[c] This list of gene-proximal variants (GPV) includes unique SNPs or deletions closer than 1.5 kb to genes, and TE insertions closer than 2 kb. All variants have been visually inspected and confirmed with IGV and/or validated via PCR. The different categories of GPV are listed

14 in the following rows. The description of the affected genes can be found in

15 **Supplementary Table S4**.

16 **Table 2**. Transposable element insertions in proximity of *AvrPm3*$^{b2/c2}$ in the 3BC mutants.

Mutant	TE class	TE name	TE distance to *AvrPm3*$^{b2/c2}$	TE description [a]
3BC_3	non-LTR retrotransposon (LINE), *RII*	*RII_Itera*	470 bp	Consensus length: 5,392 bp; number of full copies present in CHE_96224: 107 (high copy TE)
3BC_4	non-LTR retrotransposon (LINE), *RII*	*RII_Itera*	467 bp	Consensus length: 5,392 bp; number of full copies present in CHE_96224: 107 (high copy TE). 80bp from chromosome 1 inserted additionally to the *RII_Itera* element.
3BC_5	LTR retrotransposon, *Gypsy*	*RLG_Stef*	0 bp (insertion in the CDS)	Consensus length: 5,723 bp; number of full copies present in CHE_96224: 17 (low copy TE)
3BC_6	LTR retrotransposon, *Copia*	*RLC_Lily*	1,186 bp	Not detected by *detettore*, only visual analysis. Length: 5,264 bp; number of full copies present in CHE_96224: 18 (low copy TE)

17

18 [a] The consensus length indicates the length in bp of the consensus sequence of the TE,

19 retrievable from https://www.botinst.uzh.ch/en/research/genetics/thomasWicker/trep-

20 db.html. A TE was considered as a full copy when the blast hit was longer than 5,000 bp.

1 **Figure Captions**

2

3 **Figure 1**. AvrXpose pipeline to isolate gain-of-virulence *Bgt* mutants and to unravel the
4 corresponding mutated genes. The first step of AvrXpose includes the identification of *Bgt*
5 mutants with gain of virulence on a specific *R* gene. This is followed by bioinformatic
6 analyses, such as variant calling, transposable element insertion detection and coverage
7 analysis, and final visual confirmation using a genome viewer software (e.g. IGV). Variants
8 that potentially affect genes are selected. Finally, all the variants of *Bgt* mutants with the
9 same gain of virulence are compared, and variants affecting the same genes are selected.
10 These can be further studied and considered as putative avirulence components.

11

12 **Figure 2**. The 3BC mutants reveal multiple mechanisms of loss-of-function modifications
13 of *AvrPm3*$^{b2/c2}$. A) Leaves of Chul/8*Chancellor (*Pm3b*; upper leaf) and
14 Sonora/8*Chancellor (*Pm3c*; lower leaf) infected with the corresponding isolate. TE
15 insertions are represented with red boxes. The grey and blue boxes indicate the fragments
16 amplified with the different primer mixes. The representation is not to scale. B) PCR
17 amplification of the *AvrPm3*$^{b2/c2}$ promoter regions where some mutants have either a
18 deletion or a TE insertion. The expected fragment length of CHE_96224 is indicated with a
19 red arrow. C) The expression of *AvrPm3*$^{b2/c2}$ is reduced in all 3BC mutants at 2 days post-
20 infection (dpi). The expression normalized to the reference gene *GAPDH* is depicted on

21 the y-axis. Significance groups were calculated with ANOVA followed by the Tukey HSD
22 test (**Supplementary Table S11**).
23
24 **Figure 3**. The 3F+A mutants are virulent on *Pm3a* and *WTK4*, irrespective of *Bgt-646*
25 intactness. Two representatives of the 3F+A mutants, one having *Bgt-646* mutated and
26 the other not, are shown. All other identified *3F+A* mutants have comparable phenotypes;
27 **Supplementary Figure S4**. Where only the *R* gene is indicated, the corresponding NIL
28 was used. Cultivars susceptible to CHE_96224 (Kanzler, Chancellor, the *Pm1a* NIL and the
29 *Pm8* NIL) are highlighted in grey. The NILs containing *Pm3* alleles are labelled in green,
30 and the four *WTK4* containing *Ae. tauschii* lines in blue. The remaining *Pm* lines are in
31 white.
32
33 **Figure 4**. Schematic representation of the mutations within the Bgt-646 protein or its
34 regulatory region in four 3A+F mutants. The ankyrin repeat domains and the nuclear
35 localization signal (NLS) domain are represented with two dashed and a dotted rectangle,
36 respectively. The mutations in the 3F+A mutants are indicated with red lines.
37
38 **Figure 5**. *Bgt-646* has homologs with more than 70% sequence identity in different
39 powdery mildew species. Only BLAST hits with more than 97% sequence coverage were
40 considered for constructing the phylogenetic tree. *Bgt-646* is highlighted in dark yellow.
41 As an outgroup, the *Podosphaera aphanis* homologue was used.

42

43 **Figure 6**. The 3F+A mutants have a reduced expression of specific *Bgt* effector genes. As
44 a control, we tested *AvrPm3*$^{a2/f2}$ expression, which is absent in the parental isolate, 3F_1,
45 due to a large deletion and, consequently, in all 3F+A mutants. The expression normalized
46 to the reference gene *GAPDH* is depicted on the Y-axis. Four biological replicates were
47 tested. Significance and p-values were calculated with a two-sided ANOVA followed by a
48 Tukey HSD test (**Supplementary Table S11**). A significance threshold of $p<0.05$ was
49 chosen.

50

51 **Figure 7**. Model of the regulation of *Avr* expression in the different mutants. The upper
52 left panel (A) represents an avirulent *Bgt* isolate (in grey) infecting a host cell (in green).
53 *Bgt-646* (in yellow), together with a cofactor, here named *CoF6* (in orange), activates the
54 transcription of different effectors, among them the yet unknown *AvrWTK4* and *AvrPm3*^{a3},
55 which are secreted and recognized by hosts having the corresponding R proteins, WTK4,
56 Pm3f or Pm3a, respectively. On the upper right panel (B), a 3F mutant lacking *AvrPm3*$^{a2/f2}$,
57 hence not detected by *Pm3f*-containing hosts, is represented. Since it still expresses
58 *AvrPm3*^{a3}, it will activate the immune response in *Pm3a*-containing hosts. In the lower
59 panel (C), a 3F+A mutant lacking *AvrPm3*$^{a2/f2}$, as well as *Bgt-646* or *CoF6*, will not express
60 and secrete AvrWTK4 and AvrPm3^{a3}, making it unrecognizable by *Pm3f*-, *Pm3a*- or *WTK4*-
61 containing hosts.

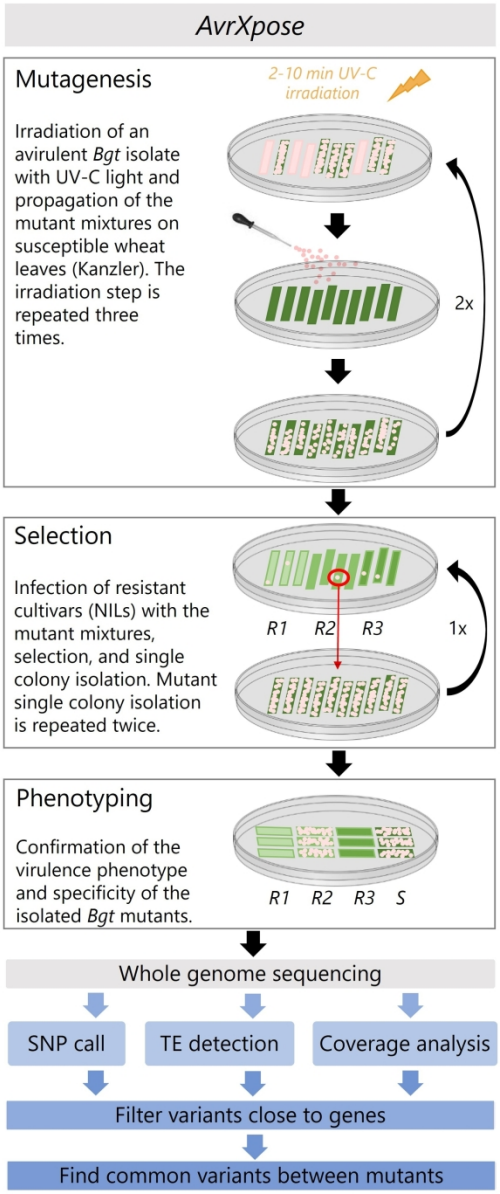

Figure 1. AvrXpose pipeline to isolate gain-of-virulence *Bgt* mutants and to unravel the corresponding mutated genes. The first step of AvrXpose includes the identification of *Bgt* mutants with gain of virulence on a specific *R* gene. This is followed by bioinformatic analyses, such as variant calling, transposable element insertion detection and coverage analysis, and final visual confirmation using a genome viewer software (e.g. IGV). Variants that potentially affect genes are selected. Finally, all the variants of *Bgt* mutants with the same gain of virulence are compared, and variants affecting the same genes are selected. These can be further studied and considered as putative avirulence components.

131x310mm (300 x 300 DPI)

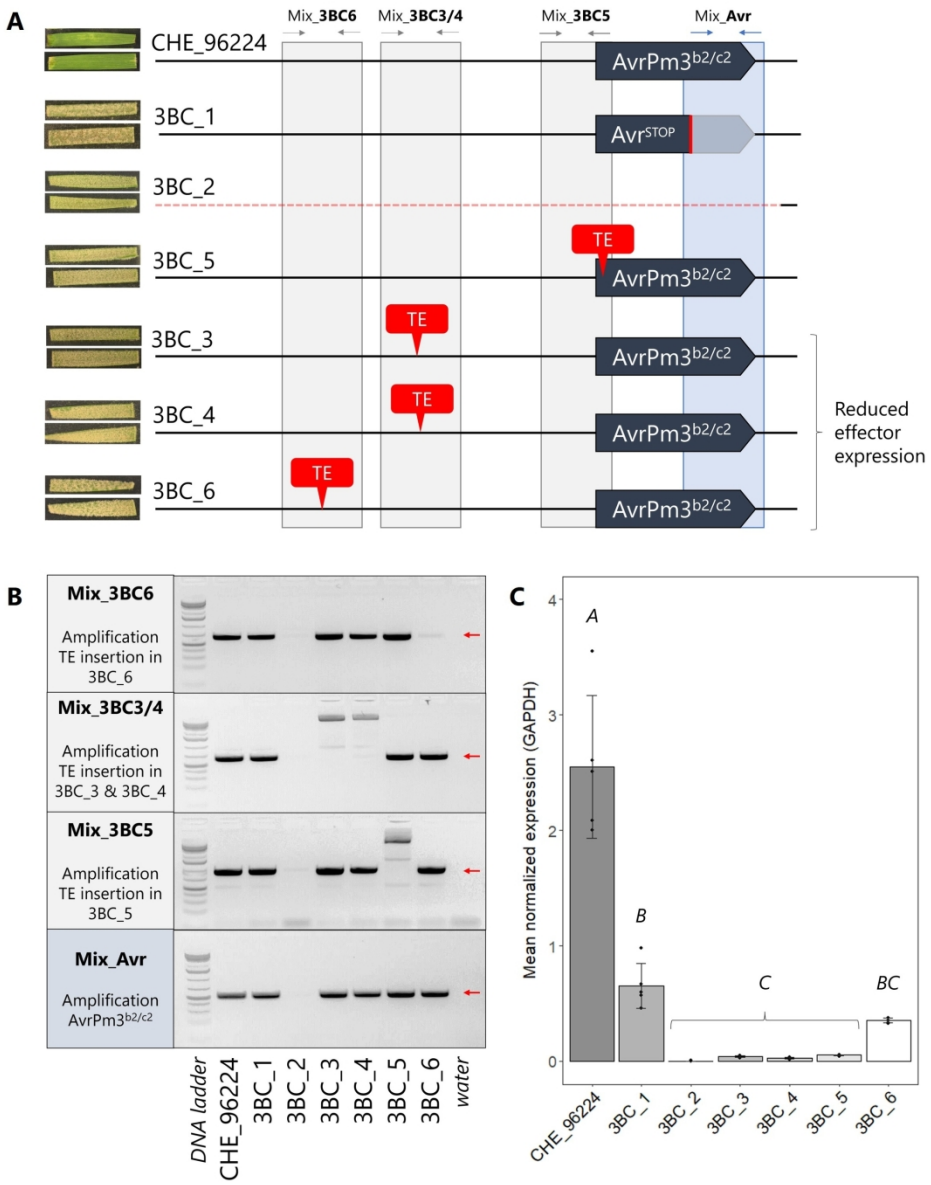

Figure 2. The 3BC mutants reveal multiple mechanisms of loss-of-function modifications of *AvrPm3*$^{b2/c2}$. A) Leaves of Chul/8*Chancellor (*Pm3b*; upper leaf) and Sonora/8*Chancellor (*Pm3c*; lower leaf) infected with the corresponding isolate. TE insertions are represented with red boxes. The grey and blue boxes indicate the fragments amplified with the different primer mixes. The representation is not to scale. B) PCR amplification of the *AvrPm3*$^{b2/c2}$ promoter regions where some mutants have either a deletion or a TE insertion. The expected fragment length of CHE_96224 is indicated with a red arrow. C) The expression of *AvrPm3*$^{b2/c2}$ is reduced in all 3BC mutants at 2 days post-infection (dpi). The expression normalized to the reference gene *GAPDH* is depicted on the y-axis. Significance groups were calculated with ANOVA followed by the Tukey HSD test (**Supplementary Table S11**).

186x235mm (300 x 300 DPI)

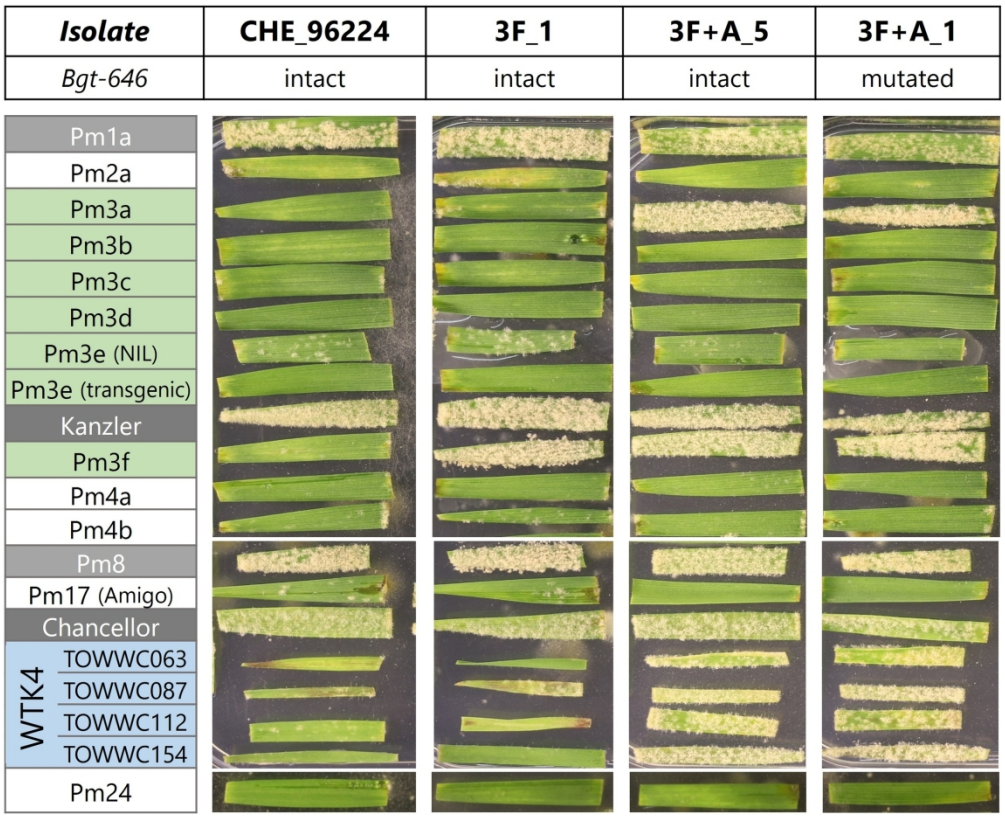

Figure 3. The 3F+A mutants are virulent on *Pm3a* and *WTK4*, irrespective of *Bgt-646* intactness. Two representatives of the 3F+A mutants, one having *Bgt-646* mutated and the other not, are shown. All other identified 3F+A mutants have comparable phenotypes; **Supplementary Figure S4**. Where only the *R* gene is indicated, the corresponding NIL was used. Cultivars susceptible to CHE_96224 (Kanzler, Chancellor, the *Pm1a* NIL and the *Pm8* NIL) are highlighted in grey. The NILs containing *Pm3* alleles are labelled in green, and the four *WTK4* containing *Ae. tauschii* lines in blue. The remaining *Pm* lines are in white.

196x160mm (300 x 300 DPI)

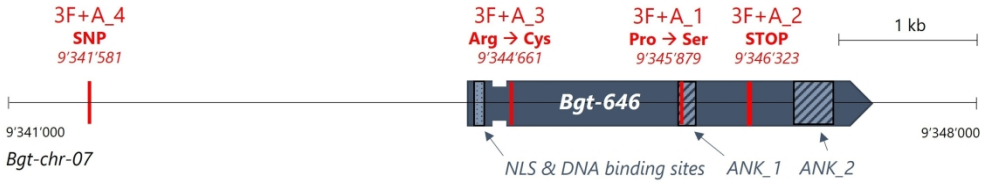

Figure 4. Schematic representation of the mutations within the Bgt-646 protein or its regulatory region in four 3A+F mutants. The ankyrin repeat domains and the nuclear localization signal (NLS) domain are represented with two dashed and a dotted rectangle, respectively. The mutations in the 3F+A mutants are indicated with red lines.

228x44mm (300 x 300 DPI)

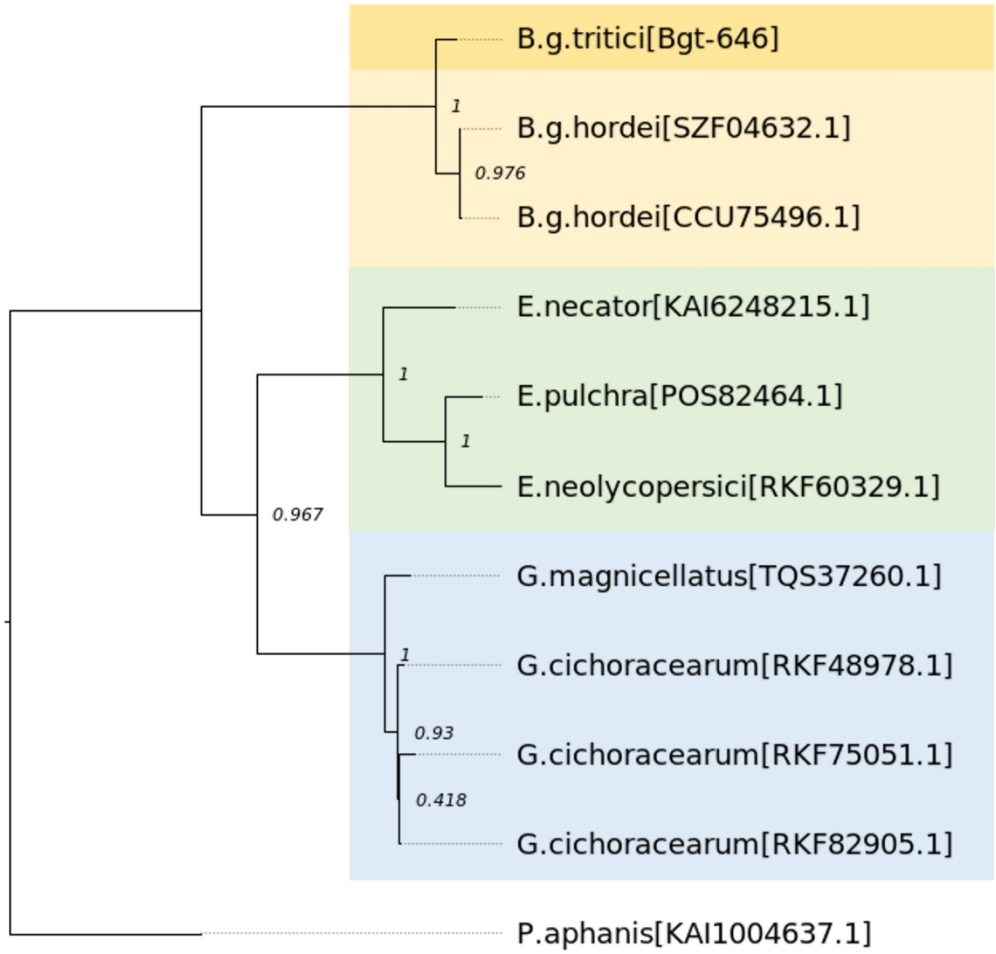

Figure 5. *Bgt-646* has homologs with more than 70% sequence identity in different powdery mildew species. Only BLAST hits with more than 97% sequence coverage were considered for constructing the phylogenetic tree. *Bgt-646* is highlighted in dark yellow. As an outgroup, the *Podosphaera aphanis* homologue was used.

242x232mm (300 x 300 DPI)

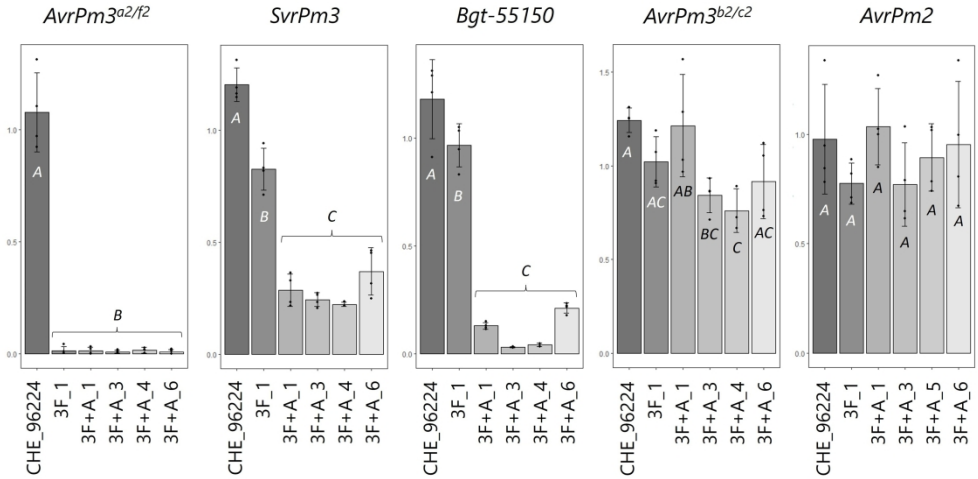

Figure 6. The 3F+A mutants have a reduced expression of specific *Bgt* effector genes. As a control, we tested *AvrPm3*$^{a2/f2}$ expression, which is absent in the parental isolate, 3F_1, due to a large deletion and, consequently, in all 3F+A mutants. The expression normalized to the reference gene *GAPDH* is depicted on the Y-axis. Four biological replicates were tested. Significance and p-values were calculated with a two-sided ANOVA followed by a Tukey HSD test (**Supplementary Table S11**). A significance threshold of $p<0.05$ was chosen.

295x145mm (300 x 300 DPI)

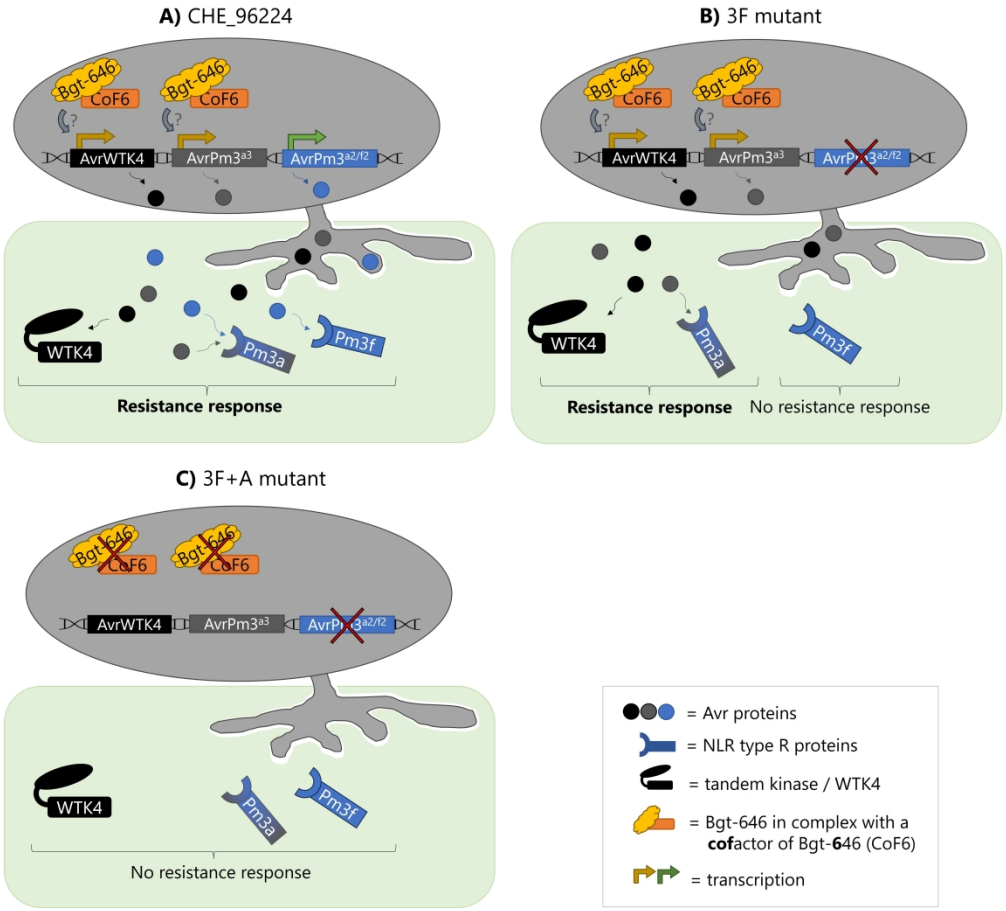

Figure 7. Model of the regulation of *Avr* expression in the different mutants. The upper left panel (A) represents an avirulent *Bgt* isolate (in grey) infecting a host cell (in green). *Bgt-646* (in yellow), together with a cofactor, here named *CoF6* (in orange), activates the transcription of different effectors, among them the yet unknown *AvrWTK4* and *AvrPm3^{a3}*, which are secreted and recognized by hosts having the corresponding R proteins, WTK4, Pm3f or Pm3a, respectively. On the upper right panel (B), a 3F mutant lacking *AvrPm3$^{a2/f2}$*, hence not detected by *Pm3f*-containing hosts, is represented. Since it still expresses *AvrPm3^{a3}*, it will activate the immune response in *Pm3a*-containing hosts. In the lower panel (C), a 3F+A mutant lacking *AvrPm3$^{a2/f2}$*, as well as *Bgt-646* or *CoF6*, will not express and secrete AvrWTK4 and AvrPm3^{a3}, making it unrecognizable by *Pm3f*-, *Pm3a*- or *WTK4*-containing hosts.

399x366mm (330 x 330 DPI)

Article title:

Mutagenesis of wheat powdery mildew reveals a single gene controlling both NLR and tandem kinase-mediated immunity

Authors:

Zoe Bernasconi, Ursin Stirnemann, Matthias Heuberger, Alexandros G. Sotiropoulos, Johannes Graf, Thomas Wicker, Beat Keller, Javier Sánchez-Martín

Table of Contents

***

Supplementary Tables S1. – S13. → *see separate Excel document*

***

Extended data. Scaffolds and sequences of 3BC mutants → *see separate Text document*

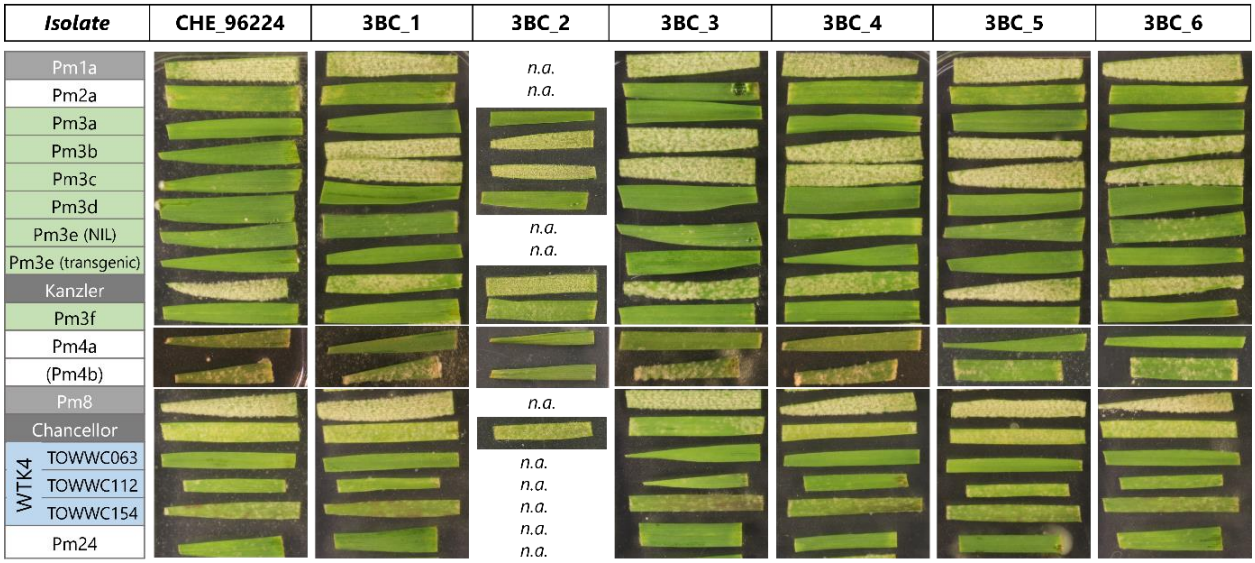

Supplementary Figure S1. Phenotyping of the 3BC mutants.

The 3BC mutants exhibit specific gain of virulence on *Pm3b* and *Pm3c* but show no virulence on other NILs for which their parental isolate CHE_96224 is avirulent. Possibly due to spore overload or seedstock contamination, all isolates (CHE_96224 and the 3BC mutants) show a slight growth on the *Pm4b* NIL, which however was not observed in repeated experiments. Mutant 3BC_2 died shortly after sequencing, therefore it was not possible to perform phenotyping on all the NILs, as done for the other mutants. Cultivars susceptible to CHE_96224 (Kanzler, Chancellor, the *Pm1a* NIL and the *Pm8* NIL) are highlighted in grey. The NILs containing *Pm3* alleles are labelled in green, and the three *WTK4* containing *Ae. tauschii* lines in blue. The remaining *Pm* lines are in white.

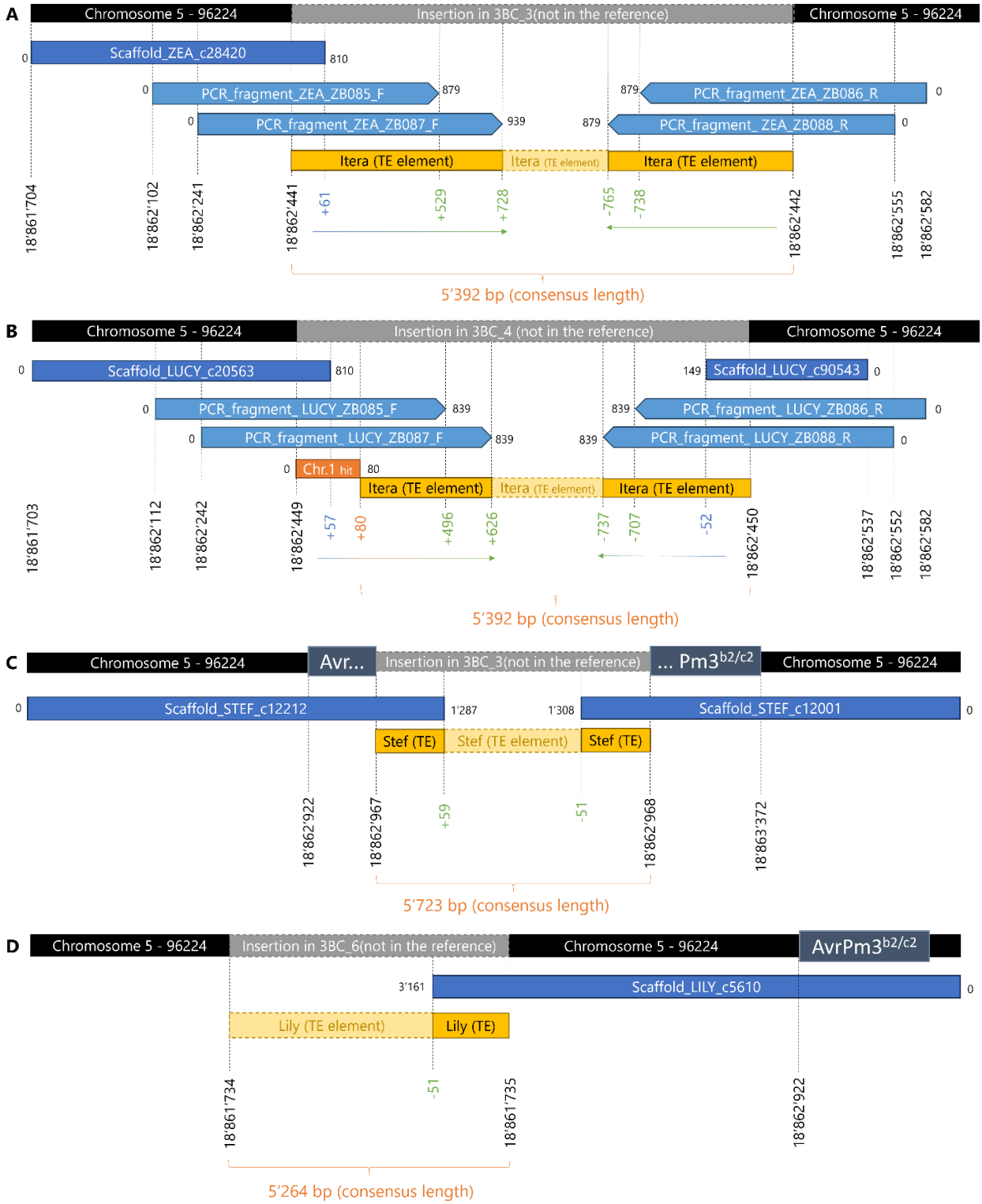

Supplementary Figure S2. De-novo assemblies of TE insertion regions – 3BC mutants. Schematic representation of the TE insertions loci close to AvrPm3$^{b2/c2}$ in mutants 3BC_3 (A), 3BC_4 (B), 3BC_5 (C) and 3BC_6 (D). In yellow are represented the different TE insertions (with the known sequence in the darker box, and the part derived from the consensus

sequence in the brighter box), in bright blue the sequences obtained with PCR and in dark blue the scaffolds of the de-novo assembly. All scaffold and PCR sequences can be found in **Extended data**.

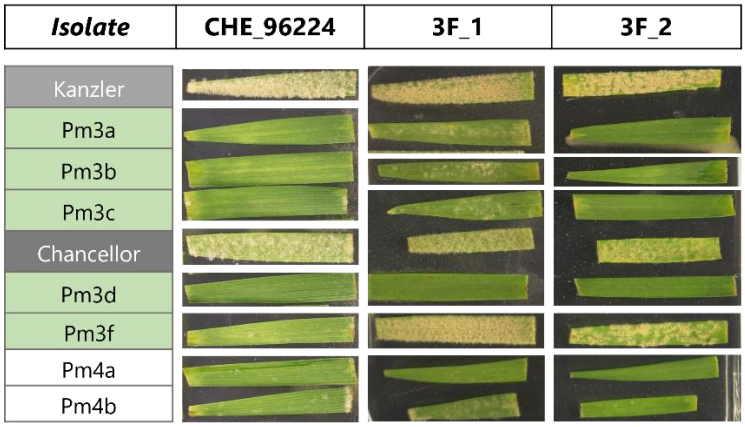

Supplementary Figure S3. Phenotyping of the 3F mutants.
The 3F mutants exhibit a specific gain of virulence on *Pm3f,* and no virulence on other NILs for which their parental isolate CHE_96224 is avirulent. Due to spore overload, mutant 3F_1 shows a slight growth on some *Pm3* and *Pm4* NILs, which however was not observed in repeated experiments (e.g. **Supplementary Figure S4**). Cultivars susceptible to CHE_96224 (Kanzler and Chancellor) are highlighted in grey. The NILs containing *Pm3* alleles are labelled in green and *Pm4* lines in white.

Isolate	**CHE_96224**	**3F_1**	**3F+A_6**	**3F+A_4**	**3F+A_2**	**3F+A_3**
Bgt-646	intact	intact	intact	*SNP in promoter*	mutated	mutated

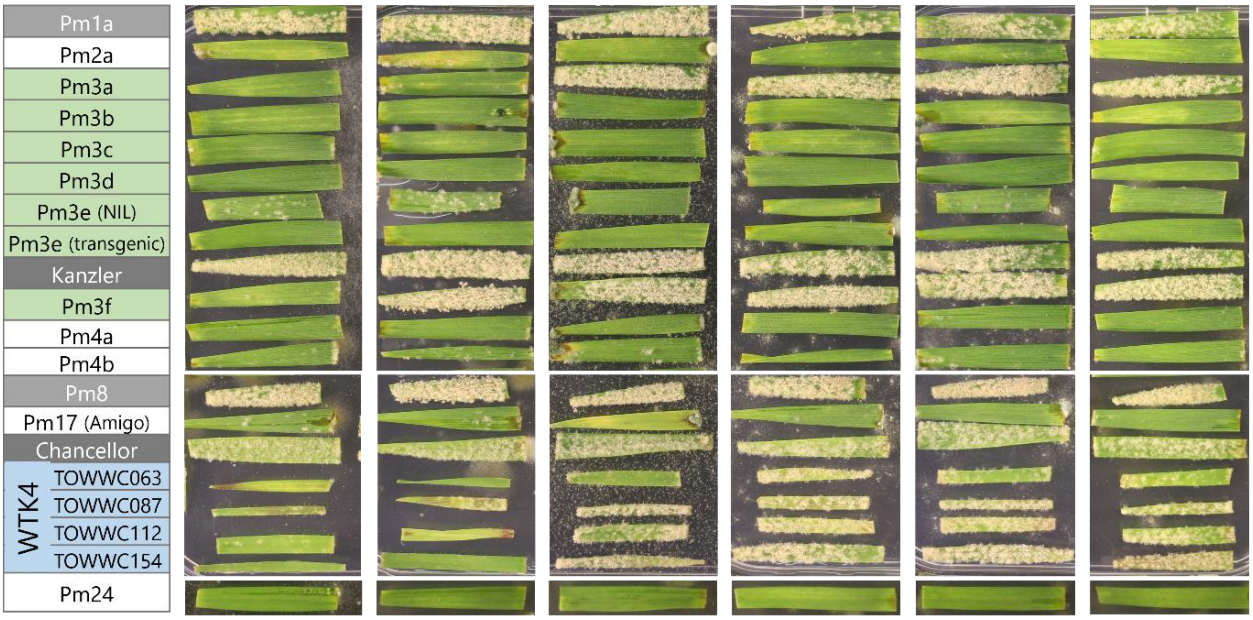

Supplementary Figure S4. Phenotyping of the 3F+A mutants.

The 3F+A mutants exhibit specific gain of virulence on *Pm3a* and *WTK4* but show no virulence on other NILs for which their parental isolate 3F_1 is avirulent. Cultivars susceptible to CHE_96224 (Kanzler, Chancellor, the *Pm1a* NIL and the *Pm8* NIL) are highlighted in grey. The NILs containing *Pm3* alleles are labelled in green, and the four *WTK4* containing *Ae. tauschii* lines in blue. The remaining *Pm* lines are in white.

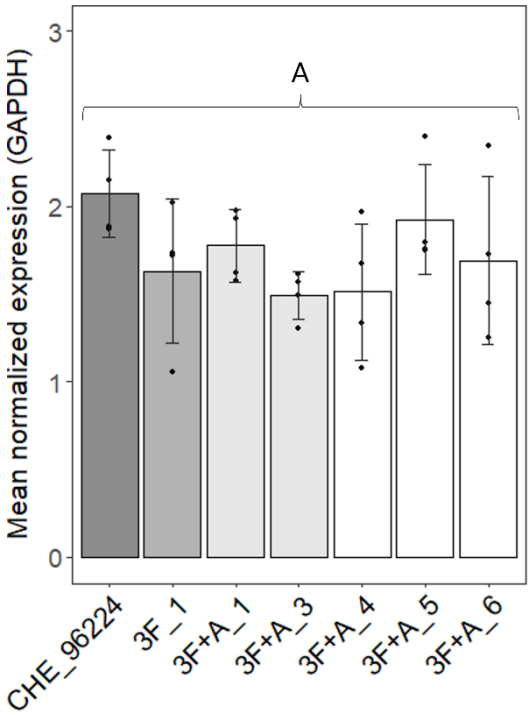

Supplementary Figure S5. *Bgt-646* expression in the 3F+A mutants.

The expression of *Bgt-646* in the 3F+A mutants was not significantly different to *Bgt-646* expression in their parental isolate 3F_1 at 2 days post infection (dpi). The expression normalized to the reference gene *GAPDH* is depicted on the Y axis. Significance and P-values were calculated through analysis of variance (ANOVA) followed by a Tukey HSD test to estimate differences in expression between *Bgt* mutants and their parental isolate 3F_1 (**Supplementary Table S11**). A significance threshold of $p<0.05$ has been chosen.

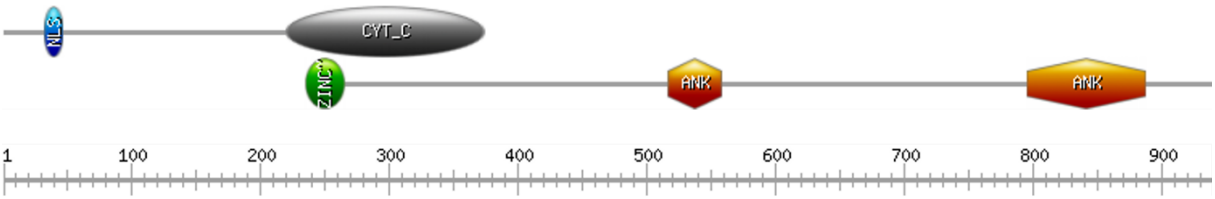

Supplementary Figure S6. Domains of *Bgt-646* predicted by ScanPROSITE.
The figure has been produced with the PROSITE online tool and is based on the predictions described in **Supplementary Table S8**.

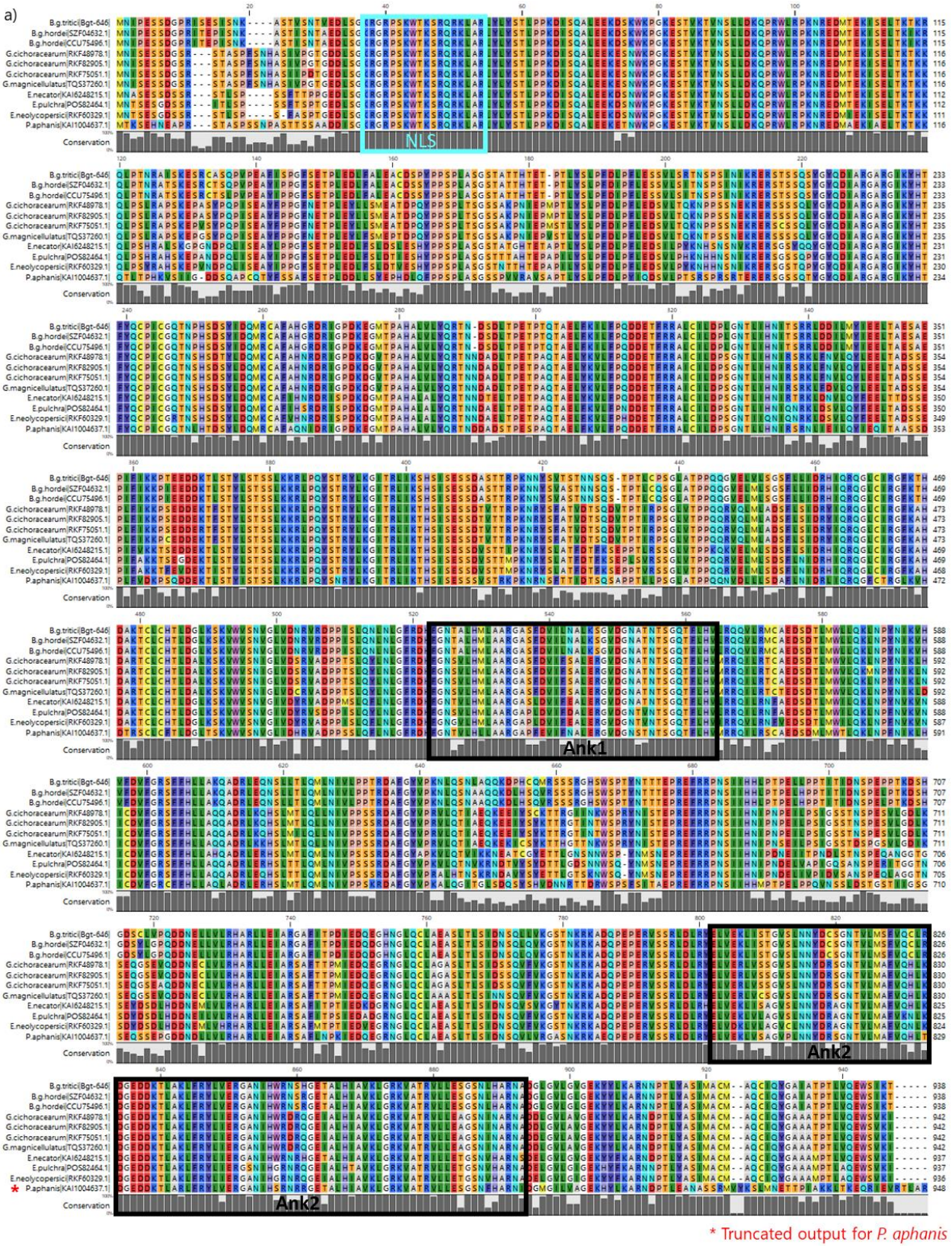

Supplementary Figure S7. Alignment of *Bgt-646* homologs.

Alignment of proteins with more than 70% protein identity with Bgt-646 using COBALT (Papadopoulos and Agarwala 2007). This alignment was used to produce the phylogenetic tree shown in **Figure 5**.

#MPMI - Bernasconi et al.
#Article Title: Mutagenesis of wheat powdery mildew reveals a single gene controlling both NLR and tandem kinase-mediated immunity
#Extended data - Scaffolds and PCR fragments in the 3BC mutants (see Supplementary Figure S2)

>Scaffold_ZEA_c28420
ATCACATATTCTCCCGATTCATATCATTATTATTCTATTCATAAAATCGC
GCCCCTATTCTTTGAGCCGCCTTACTAATCGAACCCATACCGGTTTTCCA
ACACTGAGCGATAACATCGGTAGCCCTGTAAAGTGAAAAAATAATCTTTG
TCGTCTATGTCGGGGTATAGAATACTCGAGAACATTCAGTCGGTTCCAAT
AATTTCTTCCTTTCATTTAACCTTTGAAACACGTGGTCTCTTGTGTGGTC
GAGATTCAGGAATAAGTCAATCCTTAAACGTATGATGATGAGATGCTGTC
TTTCACTTTCTAGGTTGAGCCTGTCTTGCTGTCCATCAACCGAGTACTTC
AAGATTAGGGTGGTGGGCACAATAGGAGCTTACCTGCTAAGTACTCGCGC
AACTTCAAACTAGATAAATACCCACATTCATATTGATCCTCTGGCGCAAG
TTCAATTAAACGAGACTTTTTAAAATTGATTCTTGTTTACGAGTGATACA
GAAGTGCTCGGAGCAGAATTGATATAGTATAGGGTTAAACGGAATGTGTA
TATGTCACGGCACTCATAGCACTGTAAAAACGCTGCGACCGTCTTTGTAC
TACTATGGAACTACCAATACAGGGTATACAATATCTCCAAACGCCTTACC
TCCTTACCACTTGAGTAGACCATGATCACAGTTATAGCTCCGTCATATTA
AGGTGCTGGGATGATTATTTTCGACTAACACTCTTACAATCTAACAGAAC
AACATCACATCAAGCATAGATCCCACATCATATTATCCACAACACTTCTT
ACAAGAACTT
>PCR_fragment_ZEA_ZB085
CTGCAACTTCAACTAGATAAATACCCACATTCATATTGATCCTCTGGCGCAAGTTCA
ATT
AAACGAGACTTTTTAAAATTGATTCTTGTTTACGAGTGATACAGAAGTGCTCGGAGC
AGA
ATTGATATAGTATAGGGTTAAACGGAATGTGTATATGTCACGGCACTCATAGCACTG
TAA
AAACGCTGCGACCGTCTTTGTACTACTATGGAACTACCAATACAGGGTATACAATAT
CTC
CAAACGCCTTACCTCCTTACCACTTGAGTAGACCATGATCACAGTTATAGCTCCGTC
ATA
TTAAGGTGCTGGGATGATTATTTTCGACTAACACTCTTACAATCTAACAGAACAACA
TCA
CATCAAGCATAGATCCCACATCATATTATCCACAACACTTCTTACAAGAACTTCCAT
CTG
GTGCAATGGCCCCAGCCGTTGCATCGTCATCGACAACGCCCCCGAATCCAGGGGGG
CAAC
TCCACCCAAGCCTGCTAGGCATTGTTAATGCAATGCAAAAAGCAGAACAAGAAAGA
AAAG
AAAGATTGGGCATAGCCCAGGAATTTCTTGAACTAATCGACTCCTGGGCCAAGAGC
AAAG

GAGAGAAGCAAGCAGCAGCAGTCGTCGCGACTCTGATGAACAAGATCACGCCTGTC
ATCA
CTGCCTTTGCAGTAGATCAGGCAGAAGTAATCAATAGTCCAAGTAAGAACTCCCCCG
CCA
TGGCAAGCACTCCCAAACCAGTCGCGCCTAGGAACCACATTGTTGTTGAGAACAAC
AGCC
ACGGCCTACCTCCAAAGCCGCAAGAAAAAAGCTCGCCTTGGGTTACAGTTGCTCGC
AAAG
CAGCCAAGTTACCAACACCGCCCAGTGCGCAAGTTCCGA
>PCR_fragment_ZEA_ZB086
GGTTCATTTGACCTAATGTAAACAAAAGGCTAATTATTTTCGACAGCTATGTTATAA
TAT
TCATGCAAGTTATCAAGTTTGCCCAAAATTTCAATGTTAAATTGATTAAGCTAATTTA
GA
TATATAAGATTTCTGTTAGATTTGAATTGAATTTGAATTTGAAATCTTTAACGTGACA
GG
ACGAACCCAACATCTATTTAGACGTGACACGGGTAGATGGGCCCTACGAGCTCATTG
CTA
CCTACATGACCGGCATTAAAGCCAGAAGCGACAAAAGAAAAATAAAATCACAGCA
AATGT
CTGAGTTACGGTGCCCTGCACCGTATCCCTATCTTCCAAACACCTCTCCTCTCGAGCC
AG
AAACTATCTCAGCATGGTCACTCCCACCCTGTCAGTTCTTCGGCAGACTGTAGCATC
TGC
TTATGGTTAGGAATTGGAAAAACTTCTGCCATCCCTTCTCCCCTATCATTTCCCTGAC
CC
CAGGTGGAGTCATTTTCTCACAGCTTCTCCAACGTTGCAGAGCAGGTCGGCACTCTG
AAA
AATGCCAGGGCCTTTTCTCTCGGCCACAAATGCACATCAGATCTTCATGTTCGGGGT
TGA
AACGCCGGTGGTAGTCGGCGTAGTCCCCGTGGCCTGTTCTTGCCGCAATAAGACGGT
GAT
ACGCCCATCGAGGCAGAGCCAGTTCCGGCGGTCGCTTGCAGCGCATGTAGAGGTCG
AGAT
CTTTGTATCGTTTAGGCCGATACTTCTGCCACCACTCTTCCACAAGCTTTTGGCTCCG
CA
TTTTCACTAGTCTCCCTAGAGCCGCAAAGGTCAGAATTTGCTCGTCTCCGTTGGGCG
AAG
CTGAGGTTAGTGATTGGTCATTGAGATCTCCCAGGGCTG
>PCR_fragment_ZEA_ZB087
AACGGAATGTGTATATGTCACGGCACTCATAGCACTGTAAAAACGCTGCGACCGTCT
TTG
TACTACTATGGAACTACCAATACAGGGTATACAATATCTCCAAACGCCTTACCTCCT
TAC
CACTTGAGTAGACCATGATCACAGTTATAGCTCCGTCATATTAAGGTGCTGGGATGA
TTA

TTTTCGACTAACACTCTTACAATCTAACAGAACAACATCACATCAAGCATAGATCCC
ACA
TCATATTATCCACAACACTTCTTACAAGAACTTCCATCTGGTGCAATGGCCCCAGCC
GTT
GCATCGTCATCGACAACGCCCCCGAATCCAGGGGGGCAACTCCACCCAAGCCTGCT
AGGC
ATTGTTAATGCAATGCAAAAAGCAGAACAAGAAAGAAAAGAAAGATTGGGCATAG
CCCAG
GAATTTCTTGAACTAATCGACTCCTGGGCCAAGAGCAAAGGAGAGAAGCAAGCAGC
AGCA
GTCGTCGCGACTCTGATGAACAAGATCACGCCTGTCATCACTGCCTTTGCAGTAGAT
CAG
GCAGAAGTAATCAATAGTCCAAGTAAGAACTCCCCCGCCATGGCAAGCACTCCCAA
ACCA
GTCGCGCCTAGGAACCACATTGTTGTTGAGAACAACAGCCACGGCCTACCTCCAAA
GCCG
CAAGAAAAAAGCTCGCCTTGGGTTACAGTTGCTCGCAAAGCAGCCAAGTTACCAAC
ACCG
CCCAGTGCGCAAGTTCCGAGAAGACCGGCTCCGATAAGCCGCCCTAAGGCACAGAC
AACA
CCCAAGGAAGACAAACGCCTGTTCCTTCGTTTGGGGTAGAGATCACCACTGGCACA
AATT
ATCACCAGTCACAATCAAAAAGATAATAACCGACAAGGCTGGGATAGCAGCCTCAG
CTAT
CACCTCGATGTACCCAGTCAGGTCGGGGATCGCTCTCGA
>PCR_fragment_ZEA_ZB088
GGGCTAATTATTTTCGACAGCTATGTTATAATATTCATGCAAGTTATCAAGTTTGCCC
AA
AATTTCAATGTTAAATTGATTAAGCTAATTTAGATATATAAGATTTCTGTTAGATTTG
AA
TTGAATTTGAATTTGAAATCTTTAACGTGACAGGACGAACCCAACATCTATTTAGAC
GTG
ACACGGGTAGATGGGCCCTACGAGCTCATTGCTACCTACATGACCGGCATTAAAGC
CAGA
AGCGACAAAAGAAAAATAAAATCACAGCAAATGTCTGAGTTACGGTGCCCTGCACC
GTAT
CCCTATCTTCCAAACACCTCTCCTCTCGAGCCAGAAACTATCTCAGCATGGTCACTC
CCA
CCCTGTCAGTTCTTCGGCAGACTGTAGCATCTGCTTATGGTTAGGAATTGGAAAAAC
TTC
TGCCATCCCTTCTCCCCTATCATTTCCCTGACCCCAGGTGGAGTCATTTTCTCACAGC
TT
CTCCAACGTTGCAGAGCAGGTCGGCACTCTGAAAAATGCCAGGGCCTTTTCTCTCGG
CCA
CAAATGCACATCAGATCTTCATGTTCGGGGTTGAAACGCCGGTGGTAGTCGGCGTAG
TCC

CCGTGGCCTGTTCTTGCCGCAATAAGACGGTGATACGCCCATCGAGGCAGAGCCAG
TTCC
GGCGGTCGCTTGCAGCGCATGTAGAGGTCGAGATCTTTGTATCGTTTAGGCCGATAC
TTC
TGCCACCACTCTTCCACAAGCTTTTGGCTCCGCATTTTCACTAGTCTCCCTAGAGCCG
CA
AAGGTCAGAATTTGCTCGTCTCCGTTGGGCGAAGCTGAGGTTAGTGATTGGTCATTG
AGA
TCTCCCAGGCTGATTTGGGCCAGCTTATCGGCTTCTTCG

###

>Scaffold_LUCY_c20563
TATCACATATTCTCCCGATTCATATCATTATTATTCTATTCATAAAATCG
CGCCCCTATTCTTTGAGCCGCCTTACTAATCGAACCCATACCGGTTTTCC
AACACTGAGCGATAACATCGGTAGCCCTGTAAAGTGAAAAAATAATCTTT
GTCGTCTATGTCGGGGTATAGAATACTCGAGAACATTCAGTCGGTTCCAA
TAATTTCTTCCTTTCATTTAACCTTTGAAACACGTGGTCTCTTGTGTGGT
CGAGATTCAGGAATAAGTCAATCCTTAAACGTATGATGATGAGATGCTGT
CTTTCACTTTCTAGGTTGAGCCTGTCTTGCTGTCCATCAACCGAGTACTT
CAAGATTAGGGTGGTGGGCACAATAGGAGCTTACCTGCTAAGTACTCGCG
CAACTTCAAACTAGATAAATACCCACATTCATATTGATCCTCTGGCGCAA
GTTCAATTAAACGAGACTTTTTAAAATTGATTCTTGTTTACGAGTGATAC
AGAAGTGCTCGGAGCAGAATTGATATAGTATAGGGTTAAACGGAATGTGT
ATATGTCACGGCACTCATAGCACTGTAAAAACGCTGCGACCGTCTTCGTA
CTAGTATGGAACTACCAATACAGGGTATACAATATCTCCAAACGCCTTAC
CTCCTTACCACTTGAGTAGACCATGATCACAGTTATAACTCCGTCATATT
AAGGTGCTGGGATGATTATTTTCGACTAACACTCTTACAATCTAACAGAA
ATCAAAAATTCAAATTCAAATCATCCTATGCTACAACACAACAACACAAA
CCCTCCCCCG
>Scaffold_LUCY_c90543
GCTATGTTATAATATTCATGCAAGTTATCAAGTTTGCCCAAAATTTCAATGTTAAATT
GA
TTAAGCTAATTTAGATATATAAGATTTCTGTTAGATTTGAATTTTGAATTTGAAATCT
TT
AACGTGACAGGACGAACCCAACATCTATT
>PCR_fragment_LUCY_ZB085
CTTCAACTAGATAAGTACCCACATTGCATATTGATCCTCTGGGGCAGAGGTTTAAAC
GAG
ACTTTTTAAAATTGATTCTTGTTTACGAGTGATACAGAAGTGCTCGGAGCAGAATTG
ATA
TAGAATAGGGTTAAACGGAATGTGTATATGTCACGGCACTCATAGCACTGTAAAAA
CGCT
GCGACCGTCTTTGTACTACTATGGAACTACCAATACAGGGTATACAATATCTCCAAA
CGC

CTTACCTCCTTACCACTTGAGTAGACCATGATCACAGTTATAGCTCCGTCATATTAAG
GT
GCTGGGATGATTATTTTCGACTAACACTCTTACAATCTAACAGAAATCAAAAATTCA
AAT
TCAAATCGTCCTATGCTACAACACAACAACACAAACCCTCCGCCGCAAAAGACACA
ACAT
CAAGCATAGATCCCACATCATATTATCCACAACACTTCTTACAAGAACTTCCGGCTG
GTG
CAATGGCCCCAGCCGTTGCATCGTCATCGACAACGCCCCCGAATCCAGGGGGGCAA
CTCC
ACCCAAGCCTGCTAGGCATTGTTAATGCAATGCAAAAAGCAGAACAAGAAAGAAAA
GAAA
GATTGGGCATAGCCCAGGAATTTCTTGAACTAATCGACTCCTGGGCCAAGAGCAAA
GGAG
AGAAGCGAGCAGCAGCAGTCGTCGCGACTCTGATGAACAAGATCACGCCTGTCATC
ACTG
CCTTTGCAGTAGATCAAGCAGAAGTAATCCATTAGTCCCAAGTAAGATCTCCCCCCG
CCA
TGGCAAGGCACTCCCAACCCAGTCGCGCCGTAAGAACCACAATCGTTGTTTGAGAA
CAA
>PCR_fragment_LUCY_ZB086
ATGCGGTTCATTTGACCTAATGTAAACAAAAGGCTAATTATTTTCGACAGCTATGTT
ATA
ATATTCATGCAAGTTATCAAGTTTGCCCAAAATTTCAATGTTAAATTGATTAAGCTA
ATT
TAGATATATAAGATTTCTGTTAGATTTGAATTTTGAATTTGAAATCTTTAACGTGACA
GG
ACGAACCCAACATCTATTTAGACGTGACACGGGTAGATGGGCCCTACGAGCTCATTG
CTA
CCTACATGACCGGCATTAAAGCCAGAAGCGACAAAAGAAAAATAAAATCACAGCA
AATGT
CTGAGTGACGGGGCCCTGCACCGTATCCCTATCTTCCAAACACCTCTCCTCTCGAGC
CAG
AAACTATCTCAGCATGGTCACTCCCACCCTGTCAGTTCTTCGGCAGACTGTAGCATC
TGC
TTATGGTTAGGAATTGGAAAAACTTCTGCCATCCCTTCTCCCCTATCATTTCCCTGAC
CC
CAGGTGGAGTCATTTTCTCACAGCTTCTCCAACGTTGCAGAGCAGGTCGGCACTCTG
AAA
AATGCCAGGGCCTTTTCTCTCGGCCACAAATGCACATCAGATCTTCATGTTCGGGGT
TGA
AACGCCGGAGGTAGTCGGCGTAGTCCCCGTGGCCTGTTCTTGCCGCAATAAGACAG
AGAT
ACGCCCATCGAGGCAGAGCCAGTTCCGGCGGTCGCTTGCAGCGCATGATAGAGGTC
GAGA

TCTTTGTATCGTTTAGGCCGATACTTCTGCCACCACTCTTCCACAAGCTTTTGGCTCC
GC
ATTTTTCACTAGTCTCCCTAGAGCCGCAAAGGTCAGAATTTGCTCGTCTCCGTTGGG
GA
>PCR_fragment_LUCY_ZB087
TAACGGAATGTGTATATGTCACGGCACTCATAGTACTGGAAAAACGCTGCGTATCGT
CTT
TGTACTACTATGGAACTACCAATACGGGGGATACAATATGTCCAAACGCCTTACCTC
CTT
ACCACTTGAGTAGACCATGATCACAGTTATAGCTCCGACATATTAAGGTGCTGGGAT
GAT
TATTTTCGACTAACACTCTTACAATCTAACAGAAATCATAAATTCAAATTCAAATCA
TCC
TATGCTACAACACAACAACACAAACCCTCCCCCGCAAAAAACACAACATCAAGCAT
AGAT
CCCACATCATATTATCCACAACACTTCTTACAAGAACTTCCGGCTGGCGCAATGGCC
CCA
GCCGTTGCATCCTCATCGACAACTCCCCCGAATCCAGGGGGGCAACTCCACCCAAGC
CTG
CTATGTATTGTTAATGCAATGCAAAAAGCAGAACAAGAAAGAAAAGAAAGATTGGG
CATA
GCCCAGGAATTTCTTGAACTAATCGACTCCTGGGCCAAGAGCAAAGGAGAGAAGCA
TGCA
GCAGCAGTCGTCGCGACTCTGATGAACAAGATCACGCCTGTCATCACTGCCTTTGCA
GTA
GATCAGGCAGAAGTAATCAATAGTCCAAGTAAGAACTCCCCCGCCATGGCAAGCAC
TCCC
AAACCAGTCGCGCCTAGGAACCACATTGTTGTTGAGAACAACAGCCACGGTCTACC
TCCA
AAGCCGCAAGAAAAAAGCTCGCCTTGGGTTACAGTTGCTCGCAAAGCAGCCAAGTT
ACCA
ACACCGCCCAGTGCGCAAGTTCCCGAGAACGACCGGCTCCGATAATGTCCGTCCTA
ATG
>PCR_fragment_LUCY_ZB088
CTAATCATTTTCGACAGCTATGCCATAATATTCATGCAAGCTATCAAGCAAGCCCAA
AAT
TTCAATGTTAAATTGATTAAGCTAATTTAGATATATAAGATTTCTGTTAGATTTGAAT
AT
TGAATTTGAAATCTTTAACGAGACAGGACGAACCCAACATCTATTTAGACGTGACAC
GGG
TAGATGGGCCCTACGAGCTCATTGCTACCTACATGACCGGCATGGAAGCCAGAATC
GACA
AAAGAAAAATAAAATCACAGCAAATGTCTGAGTTACGGTGCCCTGCACCGCATCCC
TATC
TTCCAAACACCTCTCCTCTCGAGCCACAAACTATCTCACCATGGTCACTCCCACCCT
GTC

AGTTCTTCGGCAGACTGTATGCATCTGCTTATGGATAGGAATTGGAAAAACTTCTGC
CAT
CCCTTCTCCCCTATCATTTCCCTGACCCCAGGTGGAGACATTTTCTCACAGCTTCTCC
AA
CTGTGCAGAGCAGGCCGGCACTCTGAAAAATGCCAAGGACTTTTCTCTCGGCCACA
AATG
CACATCAGATCTTCATGTTCGGGGTTGAAACGCCGGTGGTAGTCGGCATCATCACCG
AGG
CCTGTTCTTGCCGCAATAAGACGGAGATACGCCCATCGAGGCAGAGCCAGTTCCGG
CGGT
CGCTAGCAGCGCATGTAGAGGTCCAGATCTTTGTATCGTATAGGCCGATACTTCTGC
CAC
CACTCTTCCACAAGCTATTGGCTCCACATTTTCACTAGTCTCCCTAGAGCCGCCACCG
GT
CAGAATTTGCTCGTCTCCGCTGGGCGAACCTGGAGCTTACATGATTTGTCGATTGAA
GA

###

>Scaffold_STEF_c12001
ATGTAGTTTAGGGAAAGAATATGAGGGTGCTGCTCTATCCTCAGTTCCTG
ACAATGACTGTACTTGGCTATTTATTCTACCGGTGTGGAAACGACTACAT
TACTGAGAGAGCATTAATCAATCAAATTAGCATGGAACATAAAAAACTGA
CAGGTCAAGGGTCGAGTGCTGATAGTTTCCCAGGGGGAAGGGCAACCGCT
GAAGTAACCTTCTGGGAACCTTCTATATCGAATCCAGGTATAAACGAATC
ATTCCAAATCTATGGCATTCCCCTATAATACTTACTGGCAACAAGGTACT
TACCTCGATATCAAGGTGAAATTTGATATTTACAGACAAATGCTTTCCTT
CGAAGTTTCATCTTCGGGAAAGAGAATTCCCTGTGAGGGAGATTACGGTG
CAGAAATTCCCGAAGAGGATCTAGAGGTTTCCGACGAACCTTATTATGCC
AACTAATATTTCAGACACTATGCAACAGCATTGTAGCTTTCCAGGCAATG
TTATATAATCATCAAATCAGACAATTTTTATTGAGGTATTGAAGATATAC
GGGCTACAAAATTTTCACCATGTTGGGTCCTTGAGATGTGCTATTTCAAG
TCAATCGGCTCTATCTAGATACCACACTACTACGTCCTATGTAGCCATGT
TTACTGATAATCAAAATTTTTACCTAATCTAATGACTAATTCTTCACCAC
AATCCTTCTGTTGAAATGCTACCCATCCCTGAAAATAAAATGTCGAATGG
CCTAATGACTTAATGACCTTTCATGTATAATCTTAGATATCATGACTAAT
TATGTTGATAAGTAATGAGTTACCTGTTTAGGAATGGCGTCAGGAGAGAG
GGACAACTGCTGTATATACGTGTTTCCTTTAGCCAGAAGAGAAAGAATAG
AAGAGATATGTTTACCACCAATTGTTATTACTGCGACAGAAAGCTTGTGG
TATGAATAACACTCGAGTATTCCGACATATACTAAGAATAAGGAGAGCTC
TTCAAGTGATGACAGAGAAAAGCAAAGTATAAACTTCAAGGGGTATCTGT
AGATGTCAAATACATGTGGGACTATTCTCGACACCTGTCAGTGGTGTTCG
CTATAACCTCCAGCTCTCACTGTAGGGTCAGATCCCTACTTGTTATGAGG
GGAGCGAGGTGCGATGTTAACGTGAAGAAGAGTCTGGTGGATCAAGGTTA
GGTTTAATTGACTGAACGTGACACAATCTATATCTAGTGCGCGCTTCACT
CTGTTTGTACATGACAAGCGAGACCCTAATACTAGGGCTGTTGAGAATCC

AGCCTTGT
>Scaffold_STEF_c12212
ATTCATAAAATCGCGCCCGTATTCTTTGAGCCGCCTTACTCATCGAACCC
ATACCGGTTTTCCAACACTGAGCGATAACATCGGTAGCCCTGTAAAGTGA
AAAAATAATCTTTGTCGTCTATGTCGGGGTATAGAATACTCGAGAACATT
CAGTCGGTTCCAATAATTTCTTCCTTTCATTTAACCTTTGAAACACGTGG
TCTCTTGTGTGGTCGAGATTCAGGAATAAGTCAATCCTTAAACGTATGAT
GATGAGATGCTGTCTTTCACTTTCTAGGTTGAGCCTGTCTTGCTGTCCAT
CAACCGAGTACTTCAAGATTAGGGTGGTGGGCACAATAGGAGCTTACCTG
CTAAGTACTCGCGCAACTTCAAACTAGATAAATACCCACATTCATATTGA
TCCTCTGGCGCAAGTTCAATTAAACGAGACTTTTTAAAATTGATTCTTGT
TTACGAGTGATACAGAAGTGCTCGGAGCAGAATTGATATAGTATAGGGTT
AAACGGAATGTGTATATGTCACGGCACTCATAGCACTGTAAAAACGCTGC
GACCGTCTTCGTACTAGTATGGAACTACCAATACAGGGTATACAATATCT
CCAAACGCCTTACCTCCTTACCACTTGAGTAGACCATGATCACAGTTATA
GCTCCGTCATATTAAGGTGCTGGGATGATTATTTTCGACTAACACTCTTA
CAATCTAACAGAAATCTTATATATCTAAATTAGCTTAATCAATTTAACAT
TGAAATTTTGGGCAAACTTGATAACTTGCATGAATATTATAACATAGCTG
TCGAAAATAATTAGCCTTTTGTTTACATTAGGTCAAATGAACCCATATTC
CTTCGAGTCTCTTGGCAATTTACGTTTCCACCTCATGCCAATTTCTCATG
ATTATTGAAGATTACAAAGAGTCTAATTGAAACTAGTCGGTCGCTTTCAG
GGCCGTATAAATATCAGGTAATGAGGCAAGAAACACGATCTTCCCAATAT
CCTCCTTAACTACAGTGACATCCCCTACTATTCATTACAATCTTAACGCT
ACCAGTCTGGAATCAACATCTCCTTCTTGTGAGCAAGAGAGAAGCTGTTT
AAGCCGTGAGATCCAAGCTATCAATAAATACAATTACAATACTCAAATAT
AATCAACAATCCTCGCTCTCTGTATATTCAACATGAAAATCTCAGCTCTT
TTTTCTGTTGCAGCTCTGTTGAGCCAGTCAATGACTGTCAAACTCGAGGG
TACCAGGGGTTGTGTTTTATAGATAACTTAGAAGTGC

###

>Scaffold_LILY_c5610
TATATATACCGAGTTAGGGTAATATAACTTCACCTTTTGAGAAAGGTTTT
AATACTATTCATAAAATCGCGCCCCTATTCTTTGAGCCGCCTTACTAATC
GAACCCATACCGGTTTTCCAACACTGAGCGATAACATCGGTAGCCCTGTA
AAGTGAAAAAATAATCTTTGTCGTCTATGTCGGGGTATAGAATACTCGAG
AACATTCAGTCGGTTCCAATAATTTCTTCCTTTCATTTAACCTTTGAAAC
ACGTGGTCTCTTGTGTGGTCGAGATTCAGGAATAAGTCAATCCTTAAACG
TATGATGATGAGATGCTGTCTTTCACTTTCTAGGTTGAGCCTGTCTTGCT
GTCCATCAACCGAGTACTTCAAGATTAGGGTGGTGGGCACAATAGGAGCT
TACCTGCTAAGTACTCGCGCAACTTCAAACTAGATAAATACCCACATTCA
TATTGATCCTCTGGCGCAAGTTCAATTAAACGAGACTTTTTAAAATTGAT
TCTTGTTTACGAGTGATACAGAAGTGCTCGGAGCAGAATTGATATAGTAT
AGGGTTAAACGGAATGTGTATATGTCACGGCACTCATAGCACTGTAAAAA
CGCTGCGACCGTCTTCGTACTAGTATGGAACTACCAATACAGGGTATACA
ATATCTCCAAACGCCTTACCTCCTTACCACTTGAGTAGACCATGATCACA

GTTATAGCTCCGTCATATTAAGGTGCTGGGATGATTATTTTCGACTAACA
CTCTTACAATCTAACAGAAATCTTATATATCTAAATTAGCTTAATCAATT
TAACATTGAAATTTTGGGCAAACTTGATAACTTGCATGAATATTATAACA
TAGCTGTCGAAAATAATTAGCCTTTTGTTTACATTAGGTCAAATGAACCC
ATATTCCTTCGAGTCTCTTGGCAATTTACGTTTCCACCTCATGCCAATTT
CTCATGATTATTGAAGATTACAAAGAGTCTAATTGAAACTAGTCGGTCGC
TTTCAGGGCCGTATAAATATCAGGTAATGAGGCAAGAAACACGATCTTCC
CAATATCCTCCTTAACTACAGTGACATCCCCTACTATTCATTACAATCTT
AACGCTACCAGTCTGGAATCAACATCTCCTTCTTGTGAGCAAGAGAGAAG
CTGTTTAAGCCGTGAGATCCAAGCTATCAATAAATACAATTACAATACTC
AAATATAATCAACAATCCTCGCTCTCTGTATATTCAACATGAAAATCTCA
GCTCTTTTTTCTGTTGCAGCTCTGTTGAGCCAGTCAATGACTGTACTTGG
CTATTTATTCTACCGGTGTGGAAACGACTACATTACTGAGAGAGCATTAA
TCAATCAAATTAGCATGGAACATAAAAAACTGACAGGTCAAGGGTCGAGT
GCTGATAGTTTCCCAGGGGGAAGGGCAACCGCTGAAGTAACCTTCTGGGA
ACCTTCTATATCGAATCCAGGTATAAACGAATCATTCCAAATCTATGGCA
TTCCCCTATAATACTTACTGGCAACAAGGTACTTACCTCGATATCAAGGT
GAAATTTGATATTTACAGACAAATGCTTTCCTTCGAAGTTTCATCTTCGG
GAAAGAGAATTCCCTGTGAGGGAGATTACGGTGCAGAAATTCCCGAAGAG
GATCTAGAGGTTTCCGACGAACCTTATTATGCCAACTAATATTTCAGACA
CTATGCAACAGCATTGTAGCTTTCCAGGCAATGTTATATAATCATCAAAT
CAGACAATTTTTATTGAGGTATTGAAGATATACGGGCTACAAAATTTTCA
CCATGTTGGGTCCTTGAGATGTGCTATTTCAAGTCAATCGGCTCTATCTA
GATACCACACTACTACGTCCTATGTAGCCATGTTTACTGATAATCAAAAT
TTTTACCTAATCTAATGACTAATTCTTCACCACAATCCTTCTGTTGAAAT
GCTACCCATCCCTGAAAATAAAATGTCGAATGGCCTAATGACTTAATGAC
CTTTCATGTATAATCTTAGATATCATGACTAATTATGTTGATAAGTAATG
AGTTACCTGTTTAGGAATGGCGTCAGGAGAGAGGGACAACTGCTGTATAT
ACGTGTTTCCTTTAGCCAGAAGAGAAAGAATAGAAGAGATATGTTTACCA
CCAATTGTTATTACTGCGACAGAAAGCTTGTGGTATGAATAACACTCGAG
TATTCCGACATATACTAAGAATAAGGAGAGCTCTTCAAGTGATGACAGAG
AAAAGCAAAGTATAAACTTCAAGGGGTATCTGTAGATGTCAAATACATGT
GGGACTATTCTCGACACCTGTCAGTGGTGTTCGCTATAACCTCCAGCTCT
CACTGTAGGGTCAGATCCCTACTTGTTATGAGGGGAGCGAGGTGCGATGT
TAACGTGAAGAAGAGTCTGGTGGATCAAGGTTAGGTTTAATTGACTGAAC
GTGACACAATCTATATCTAGTGCGCGCTTCACTCTGTTTGTACATGACAA
GCGAGACCCTAATACTAGGGCTGTTGAGAATCCAGCCTTGTGAATCAGGC
CTACGTGAACTAAAATCTAATCAAATTCCAACTCATGCAATTTTTTGAA
ATTCGAATTTTCGAATCTTCACCTTTTTCCCGTCTCCCTCCCTCACGCGC
TCGTCGCATTCTATCAAAAAAATTGTGATCGAGTCACTGGCATTTTCACC
ATGCCACCTGTTCGAAAAAAGCGTCCCAACGCCAAGTTGGACAACACGAG
AGTCCACCCGAGGGCTCTCGAGCAATTACCTGGCCTTGCCTAGTCTCCGA
AATGCGCGGAGATGAGCAAGGTCTCCATCAAAGGGAAGGAAGAAGCCCTC
CCCGCCGTCGCTGAACCCGATACTGACATGATCGGGTCAGTCGAAATTGT
TGAGGAAATCTCTCAGCGACCCTCCGTCCCCCACAGGATTGAAGAATCGT
CCAAACCTCCTCCGACCACCTCAAAACCGTCGGAAAATGCTGCACCCATA

GCAGCATCAACATCAACGTCGCAGCTTAAAGCTGCCACGAAACCAGAGTG
TCCCCTCGAGCTACGACCAATAGTCGAAGCTGAACAACGACGCGCCGCCG
AAATAACGGCAAATCTGGCCCTCTGCTCCGCCGCCATCTCTGGCGTCGAA
GCCACCCTTCT